


Article

# Reliability Inferences of the Inverted NH Parameters via Generalized Type-II Progressive Hybrid Censoring with Applications

Ahmed Elshahhat <sup>1,\*</sup> , Heba S. Mohammed <sup>2</sup> and Osama E. Abo-Kasem <sup>3</sup><sup>1</sup> Faculty of Technology and Development, Zagazig University, Zagazig 44519, Egypt<sup>2</sup> Department of Mathematical Sciences, College of Science, Princess Nourah bint Abdulrahman University, P.O. Box 84428, Riyadh 11671, Saudi Arabia<sup>3</sup> Department of Statistics, Faculty of Commerce, Zagazig University, Zagazig 44519, Egypt

\* Correspondence: aelshahhat@ftd.zu.edu.eg

**Abstract:** Generalized progressive hybrid censored mechanisms have been proposed to reduce the test duration and to save the cost spent on testing. This paper considers the problem of estimating the unknown model parameters and the reliability time functions of the new inverted Nadarajah–Haghighi (NH) distribution under generalized Type-II progressive hybrid censoring using the maximum likelihood and Bayesian estimation approaches. Utilizing the normal approximation of the frequentist estimators, the corresponding approximate confidence intervals of unknown quantities are also constructed. Using independent gamma conjugate priors under the symmetrical squared error loss, the Bayesian estimators are developed. Since the joint likelihood function is obtained in complex form, the Bayesian estimators and their associated highest posterior density intervals cannot be obtained analytically but can be evaluated via Monte Carlo Markov chain techniques. To select the optimum censoring scheme among different censoring plans, five optimality criteria are used. Finally, to explain how the proposed methodologies can be applied in real situations, two applications representing the failure times of electronic devices and deaths from the coronavirus disease 2019 epidemic in the United States of America are analyzed.

**Keywords:** inverted NH model; generalized type-II progressive hybrid censoring; Bayesian and frequentist estimators; Metropolis–Hastings algorithm; optimum progressive censoring plan



**Citation:** Elshahhat, A.; Mohammed, H.S.; Abo-Kasem, O.E. Reliability Inferences of the Inverted NH Parameters via Generalized Type-II Progressive Hybrid Censoring with Applications. *Symmetry* **2022**, *14*, 2379. <https://doi.org/10.3390/sym14112379>

Academic Editors: Piao Chen, Ancha Xu and Juan Luis García Guirao

Received: 4 October 2022

Accepted: 4 November 2022

Published: 10 November 2022

**Publisher's Note:** MDPI stays neutral with regard to jurisdictional claims in published maps and institutional affiliations.



**Copyright:** © 2022 by the authors. Licensee MDPI, Basel, Switzerland. This article is an open access article distributed under the terms and conditions of the Creative Commons Attribution (CC BY) license (<https://creativecommons.org/licenses/by/4.0/>).

## 1. Introduction

Today, reliability technology plays a very important role, because it measures the ability of a system to successfully perform its intended function under predetermined conditions for a specified period. In this framework, several studies on system reliability have been conducted (among others, see Chen et al. [1], Xu et al. [2], Hu and Chen [3], and Luo et al. [4]). Progressive Type-II censoring (PCS-T2) has been discussed quite extensively in the literature as a highly flexible censoring scheme (for details, see Balakrishnan and Cramer [5]). At time  $T = 0$ ,  $n$  independent units are placed in a test in which the number of failures to be observed  $r$  and the progressive censoring  $\underline{R} = (R_1, R_2, \dots, R_r)$ , where  $n = \sum_{i=1}^r R_i + r$ , are determined. At the time of the first failure observed (say  $X_{1:r:n}$ ),  $R_1$  of the remaining surviving units  $n - 1$  are randomly selected and removed from the test. Similarly, at the time of the second failure (say  $X_{2:r:n}$ ),  $R_2$  of  $n - R_1 - 2$  are randomly selected and removed from the test, and so on. At the time of the  $r$ th failure (say  $X_{r:r:n}$ ), all remaining survival units  $R_r = n - r - \sum_{j=1}^{r-1} R_j$  are withdrawn from the test. However, when the experimental units are highly reliable, PCS-T2 may take a longer time to continue, and this is the main drawback of this censoring scheme. To overcome this drawback, Kundu and Joarder [6] proposed the progressive Type-I hybrid censoring scheme (PHCS-T1), which is a mixture of PCS-T2 and classical Type-I censoring.

Under PHCS-T1, the experimental time cannot exceed  $T$ . In addition, the disadvantage of PHCS-T1 is that there may be very few failures that occur before time  $T$ , and thus the maximum likelihood estimators (MLEs) may not always exist. Therefore, to handle this problem, Childs et al. [7] proposed the progressive Type-II hybrid censoring scheme (PHCS-T2). Under PHCS-T2, the experiment stops at  $T^* = \max\{X_{r:r:n}, T\}$ . Although PHCS-T2 guarantees a specified number of failures, it might take a long time to observe  $r$  failures. Therefore, Lee et al. [8] introduced the generalized progressive Type-II hybrid censoring scheme (GPHCS-T2). Suppose the integer  $r$  and the two thresholds  $T_i, i = 1, 2$  are pre-assigned such that  $r \leq n$  and  $0 < T_1 < T_2 < \infty$ . Let  $d_1$  and  $d_2$  denote the number of failures up to times  $T_1$  and  $T_2$ , respectively. At  $X_{1:r:n}, R_1$  of  $n - 1$  are withdrawn from the test at random. Following  $X_{2:r:n}, R_2$  of  $n - R_1 - 2$  are withdrawn, and so on. According to the termination time  $T^* = \max\{T_1, \min\{X_{r:r:n}, T_2\}\}$ , all remaining units are removed, and the experiment is stopped. It is useful to note that GPHCS-T2 modifies PHCS-T2 by guaranteeing that the test is completed at a predetermined time  $T_2$ . Therefore,  $T_2$  represents the absolute longest that the researcher is willing to allow the experiment to continue. The schematic diagram shown in Figure 1 represents that if  $X_{r:n} < T_1$ , then we continue to observe failures, but without any further withdrawals up to time  $T_1$  (Case-I) (i.e.,  $R_r = R_{r+1} = \dots = R_{d_1} = 0$ ); if  $T_1 < X_{r:n} < T_2$ , we terminate the test at  $X_{r:r:n}$  (Case-II); otherwise, we terminate the test at time  $T_2$  (Case-III). Thus, an experimenter will observe one of the following three data forms:

$$\{\underline{X}, \underline{R}\} = \begin{cases} \{(X_{1:r:n}, R_1), \dots, (X_{r-1:r:n}, R_{r-1}), (X_{r:r:n}, 0), \dots, (X_{d_1:n}, 0)\}; & \text{Case-I,} \\ \{(X_{1:r:n}, R_1), \dots, (X_{d_1:n}, R_{d_1}), \dots, (X_{r-1:r:n}, R_{r-1}), (X_{r:r:n}, R_r)\}; & \text{Case-II,} \\ \{(X_{1:r:n}, R_1), \dots, (X_{d_1:n}, R_{d_1}), \dots, (X_{d_2-1:n}, R_{d_2-1}), (X_{d_2:n}, R_{d_2})\}; & \text{Case-III.} \end{cases}$$

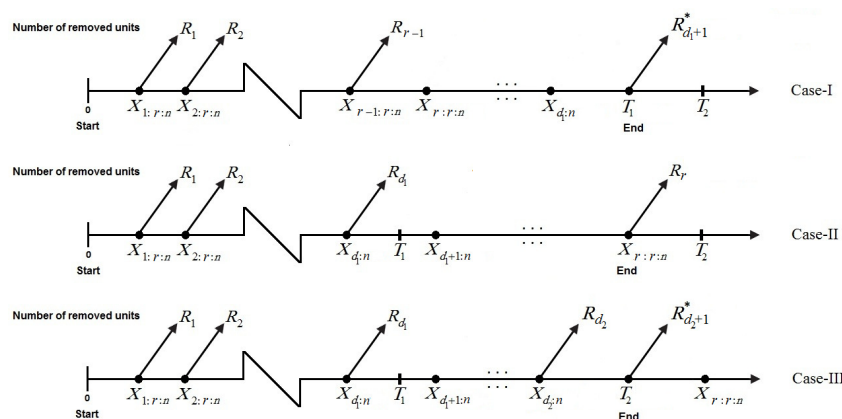


Figure 1. Diagram of GPHCS-T2.

Assume that  $\{\underline{X}, \underline{R}\}$  denotes the corresponding lifetimes from a distribution with a cumulative distribution function (CDF)  $F(\cdot)$  and probability density function (PDF)  $f(\cdot)$ . Thus, the combined likelihood function of GPHCS-T2 can be expressed as

$$L_\rho(\theta|\underline{X}) = C_\rho \prod_{j=1}^{D_\rho} f(x_{j:r:n}; \theta) [1 - F(x_{j:r:n}; \theta)]^{R_j} \Psi_\rho(T_\tau; \theta), \tag{1}$$

where  $\tau = 1, 2, \rho = 1, 2, 3$  refer to Case-I, II, and III, respectively, and  $\Psi_\rho(\cdot)$  is a composite form of the reliability functions. The GPHCS-T2 notations from Equation (1) are listed in Table 1. Additionally, from Equation (1), different censoring plans can be obtained as special cases:

- PHCS-T1 by setting  $T_1 \rightarrow 0$ ;
- PHCS-T2 by setting  $T_2 \rightarrow \infty$ ;
- Hybrid Type-I censoring by setting  $T_1 \rightarrow 0, R_j = 0, j = 1, 2, \dots, r - 1, R_r = n - r$ ;

- Hybrid Type-II censoring by setting  $T_2 \rightarrow \infty, R_j = 0, j = 1, 2, \dots, r - 1, R_r = n - r$ ;
- Type-I censoring by setting  $T_1 = 0, r = 1, R_j = 0, j = 1, 2, \dots, r - 1, R_r = n - r$ ;
- Type-II censoring by setting  $T_1 = 0, T_2 \rightarrow \infty, R_j = 0, j = 1, 2, \dots, r - 1, R_r = n - r$ .

**Table 1.** The GPHCS-T2 notations.

$\rho$	$C_\rho$	$D_\rho$	$\Psi_\rho(T_\tau; \theta)$	$R_{d_\tau+1}^*$
1	$\prod_{j=1}^{d_1} \sum_{i=j}^r (R_i + 1)$	$d_1$	$[1 - F(T_1)]^{R_{d_1+1}^*}$	$n - d_1 - \sum_{i=1}^{r-1} R_i$
2	$\prod_{j=1}^r \sum_{i=j}^r (R_i + 1)$	$r$	1	0
3	$\prod_{j=1}^{d_2} \sum_{i=j}^r (R_i + 1)$	$d_2$	$[1 - F(T_2)]^{R_{d_2+1}^*}$	$n - d_2 - \sum_{i=1}^{d_2} R_i$

Various studies based on GPHCS-T2 have also been conducted. For example, Ashour and Elshahhat [9] obtained the maximum likelihood and Bayes estimators of the Weibull parameters. Ateya and Mohammed [10] discussed the prediction problem of future failure times from the Burr-XII distribution. Seo [11] proposed an objective Bayesian analysis with partial information for the Weibull distribution. Cho and Lee [12] studied the competing risks from exponential data, and recently, Nagy et al. [13] investigated both the point and interval estimates of the Burr-XII parameters.

Nadarajah and Haghghi [14] introduced a generalization form of the exponential distribution called the Nadarajah–Haghghi (NH) distribution. Its density allows decreasing and unimodal shapes while the hazard rate exhibits increasing, decreasing, and constant shapes. Moreover, its density, survival, and hazard rate functions has two parameters, as in the Weibull, gamma and generalized exponential lifetime models. They also showed that the NH model can be interpreted as a truncated Weibull distribution. A new two-parameter inverse distribution, called the inverted Nadarajah–Haghghi (INH) distribution, for data modeling with decreasing and upside-down bathtub-shaped hazard rates as well as a decreasing and unimodal (right-skewed) density was introduced by Tahir et al. [15]. A lifetime random variable  $X$  is said to have INH distribution, where  $X \sim \text{INH}(\alpha, \delta)$ , and its PDF ( $f(\cdot)$ ), CDF ( $F(\cdot)$ ), reliability function (RF),  $R(\cdot)$ , and hazard function (HF),  $h(\cdot)$  at a mission time  $t$  are given, respectively, by

$$f(x; \alpha, \delta) = \alpha \delta x^{-2} (1 + \delta x^{-1})^{\alpha-1} \exp(1 - (1 + \delta x^{-1})^\alpha); \quad x > 0, \quad (2)$$

$$F(x; \alpha, \delta) = \exp(1 - (1 + \delta x^{-1})^\alpha); \quad x > 0, \quad (3)$$

$$R(t; \alpha, \delta) = 1 - \exp(1 - (1 + \delta t^{-1})^\alpha); \quad t > 0, \quad (4)$$

and

$$h(t; \alpha, \delta) = \frac{\alpha \delta t^{-2} (1 + \delta t^{-1})^{\alpha-1}}{\exp((1 + \delta t^{-1})^\alpha) - 1}; \quad t > 0, \quad (5)$$

where  $\alpha > 0$  and  $\delta > 0$  are the shape and scale parameters, respectively. By setting  $\alpha = 1$  in Equation (2), the inverted exponential distribution is introduced as a special case. Tahir et al. [15] showed that the proposed distribution is highly flexible for modeling real data sets that exhibit decreasing and upside-down bathtub hazard shapes. Recently, from the times until breakdown of an insulating fluid between 19 electrodes recorded at 34 kV, Elshahhat and Rastogi [16] showed that the INH distribution is the best compared with other 10 inverted models in the literature.

To the best of our knowledge, we have not come across any work related to estimation of the model parameters or survival characteristics of the new INH lifetime model in the presence of data obtained from the generalized Type-II progressive hybrid censoring plan. Therefore, to close this gap, our objectives in this study are the following. First, we derive the likelihood inference for the unknown INH parameters  $\alpha$  and  $\delta$  or any function of them, such as  $R(t)$  or  $h(t)$ . From the squared error (SE) loss, the second objective is to develop the Bayes estimates for the same unknown parameters by utilizing independent

gamma priors. In addition, based on the proposed estimation methods, the approximate confidence intervals (ACIs) and highest posterior density (HPD) interval estimators for the unknown parameters of the INH distribution, are found. Since the theoretical results of  $\alpha$  and  $\delta$  obtained by the proposed estimation methods cannot be expressed in closed form, in the  $\mathcal{R}$  programming language, the ‘maxLik’ (proposed by Henningsen and Toomet [17]) and ‘coda’ (proposed by Plummer et al. [18]) packages are used to calculate the acquired estimates. Using five optimality criteria, the third objective is to obtain the best progressive censoring plan. Using various combinations of the total sample size, effective sample size, threshold times, and progressive censoring, the efficiencies of the various estimators are compared via a Monte Carlo simulation. The estimators, thus obtained, are compared on the basis of their simulated root mean squared errors (RMSEs), mean relative absolute biases (MRABs), and average confidence lengths (ACLs). In addition, two different real data sets coming from the engineering and clinical fields are examined to see how the proposed methods can perform in practice and adopt the optimal censoring plan.

The rest of the paper is organized as follows. The maximum likelihoods and Bayes inferences of the unknown parameters and reliability characteristics are discussed in Sections 2 and 3, respectively. The asymptotic and credible intervals are constructed in Section 4. The Monte Carlo simulation results are reported in Section 5. The optimal progressive censoring plans are discussed in Section 6. Two real-life data analyses are investigated in Section 7. Finally, we conclude the paper in Section 8.

## 2. Likelihood Estimators

Suppose  $\underline{X} = \{(X_{1:r:n}, R_1), \dots, (X_{d_1:n}, R_{d_1}), \dots, (X_{d_2:n}, R_{d_2})\}$  is a GPHCS-T2 sample of a size  $d_2$  from  $\text{INH}(\alpha, \delta)$ . By substituting Equations (2) and (3) into Equation (1), where  $x_j$  is used instead of  $x_{j:r:n}$ , the likelihood function of GPHCS-T2 (1) can be written as

$$L_\rho(\alpha, \delta | \underline{X}) \propto \prod_{j=1}^{D_\rho} \alpha \delta x_j^{-2} (\psi(\delta; x_j))^{\alpha-1} e^{1-(\psi(\delta; x_j))^\alpha} [1 - e^{1-(\psi(\delta; x_j))^\alpha}]^{R_j} \Psi_\rho(T_\tau; \alpha, \delta), \quad (6)$$

where  $\psi(\delta; x_j) = (1 + \delta x_j^{-1})$ ,  $\Psi_1(T_1; \alpha, \delta) = [1 - \exp(1 - (1 + \delta T_1^{-1})^\alpha)]^{R_{d_1+1}^*}$ ,  $\Psi_2(T_\tau; \alpha, \delta) = 1$  and  $\Psi_3(T_2; \alpha, \delta) = [1 - \exp(1 - (1 + \delta T_2^{-1})^\alpha)]^{R_{d_2+1}^*}$ .

The corresponding log-likelihood function  $\ell_\rho(\cdot) \propto \ln L_\rho(\cdot)$  of Equation (6) becomes

$$\begin{aligned} \ell_\rho(\alpha, \delta | \underline{X}) \propto & D_\rho \ln(\alpha \delta) + (\alpha - 1) \sum_{j=1}^{D_\rho} \ln(\psi(\delta; x_j)) + \sum_{j=1}^{D_\rho} \left(1 - (\psi(\delta; x_j))^\alpha\right) \\ & + \sum_{j=1}^{D_\rho} R_j \ln(1 - e^{1-(\psi(\delta; x_j))^\alpha}) + W_\rho(T_\tau; \alpha, \delta), \end{aligned} \quad (7)$$

where  $W_1(T_1; \alpha, \delta) = R_{d_1+1}^* \ln \Psi_1(T_1; \alpha, \delta)$ ,  $W_2(T_\tau; \alpha, \delta) = 0$  and  $W_3(T_2; \alpha, \delta) = R_{d_2+1}^* \ln \Psi_3(T_2; \alpha, \delta)$  for Case-I, II, and III, respectively.

By differentiating Equation (7) partially with respect to  $\alpha$  and  $\delta$ , the following two likelihood equations must be solved simultaneously after equating them to zero to obtain the MLEs  $\hat{\alpha}$  and  $\hat{\delta}$ :

$$\begin{aligned} \frac{D_\rho}{\alpha} + \sum_{j=1}^{D_\rho} \ln(\psi(\delta; x_j)) - \sum_{j=1}^{D_\rho} \left( (\psi(\delta; x_j))^\alpha \ln \psi(\delta; x_j) \right) \\ + \sum_{j=1}^{D_\rho} R_j (\psi(\delta; x_j))^\alpha \ln(\psi(\delta; x_j)) F(x_j; \alpha, \delta) [1 - F(x_j; \alpha, \delta)]^{-1} + \frac{\partial W_\rho(T_\tau; \alpha, \delta)}{\partial \alpha} \Big|_{(\hat{\alpha}, \hat{\delta})} = 0, \end{aligned} \quad (8)$$

and

$$\begin{aligned} \frac{D_\rho}{\delta} + (\alpha - 1) \sum_{j=1}^{D_\rho} \psi'_\delta(\delta; x_j) - \alpha \sum_{j=1}^{D_\rho} \psi'_\delta(\delta; x_j) (\psi(\delta; x_j))^{\alpha-1} \\ + \alpha \sum_{j=1}^{D_\rho} R_j \psi'_\delta(\delta; x_j) (\psi(\delta; x_j))^{\alpha-1} F(x_j; \alpha, \delta) [1 - F(x_j; \alpha, \delta)]^{-1} + \frac{\partial W_\rho(T_\tau; \alpha, \delta)}{\partial \delta} \Big|_{(\hat{\alpha}, \hat{\delta})} = 0, \end{aligned} \quad (9)$$

where  $\psi'_\delta(\delta; x_j) = x_j^{-1}$ ,  $j = 1, 2, \dots, D_\rho$ ,  $\psi'_\delta(\delta; T_\tau) = T_\tau^{-1}$ ,  $\psi(\delta; T_\tau) = (1 + \delta T_\tau^{-1})$  such that

$$\frac{\partial W_\rho(T_\tau; \alpha, \delta)}{\partial \alpha} = \frac{(\psi(\delta; T_\tau))^\alpha \ln(\psi(\delta; T_\tau)) F(T_\tau; \alpha, \delta) R_{D_\rho+1}^*}{1 - F(T_\tau; \alpha, \delta)},$$

$$\frac{\partial W_\rho(T_\tau; \alpha, \delta)}{\partial \delta} = \frac{\alpha \psi'_\delta(\delta; T_\tau) (\psi(\delta; T_\tau))^{\alpha-1} F(T_\tau; \alpha, \delta) R_{D_\rho+1}^*}{1 - F(T_\tau; \alpha, \delta)}$$

and

$$\frac{\partial W_2(T_\tau; \alpha, \delta)}{\partial \alpha} = \frac{\partial W_2(T_\tau; \alpha, \delta)}{\partial \delta} = 0, \text{ for } \rho = 1, 3, \tau = 1, 2.$$

From Equations (8) and (9), it is clear that we have a system of two nonlinear equations which must be simultaneously satisfied to obtain the MLEs  $\hat{\alpha}$  and  $\hat{\delta}$  of  $\alpha$  and  $\delta$  in the INH model, respectively. Therefore, a closed-form solution for  $\hat{\alpha}$  and  $\hat{\delta}$  does not exist and cannot be computed analytically. Therefore, for any given GPHCS-T2 data set, a numerical methods such as the Newton–Raphson iterative method can be used to calculate  $\hat{\alpha}$  and  $\hat{\delta}$ . Once the estimates of  $\hat{\alpha}$  and  $\hat{\delta}$  are obtained, by replacing  $\alpha$  and  $\delta$  with  $\hat{\alpha}$  and  $\hat{\delta}$ , the MLEs  $\hat{R}(t)$  and  $\hat{h}(t)$  of  $R(t)$  and  $h(t)$ , respectively, can be easily derived.

### 3. Bayes Estimators

In this section, based on the SE loss function, the Bayes estimators and associated HPD intervals of  $\alpha$ ,  $\delta$ ,  $R(t)$ , and  $h(t)$  are developed. To establish this purpose, both INH parameters,  $\alpha$  and  $\delta$ , are assumed to be independently distributed as gamma priors such as  $G_\alpha(a_1, b_1)$  and  $G_\delta(a_2, b_2)$ , respectively. Several reasons to consider gamma priors are that: (1) they provide various shapes based on parameter values, (2) they are flexible in nature, and (3) they are fairly straightforward, concise, and may not lead to a result with a complex estimation issue. Then, the joint prior density of  $\alpha$  and  $\delta$  is

$$\pi(\alpha, \delta) \propto \alpha^{a_1-1} \delta^{a_2-1} \exp(-(\alpha b_1 + \delta b_2)), \quad (10)$$

where  $a_i > 0$  and  $b_i > 0$  for  $i = 1, 2$  are assumed to be known. By combining Equations (6) and (10), the joint posterior PDF of  $\alpha$  and  $\delta$  becomes

$$\pi_\rho(\alpha, \delta | \underline{X}) = C^{-1} \alpha^{D_\rho+a_1-1} \delta^{D_\rho+a_2-1} e^{-(\alpha b_1 + \delta b_2)} \Psi_\rho(T_\tau; \alpha, \delta) \times \prod_{j=1}^{D_\rho} (\psi(\delta; x_j))^{\alpha-1} e^{1-(\psi(\delta; x_j))^\alpha} [1 - e^{1-(\psi(\delta; x_j))^\alpha}]^{R_j}, \quad (11)$$

where  $C$  is the normalizing constant. Subsequently, the Bayes estimate  $\tilde{\varphi}(\cdot)$  of any function of  $\alpha$  and  $\delta$ , such as  $\varphi(\alpha, \delta)$ , under SE loss is the posterior expectation of Equation (11), which is given by

$$\tilde{\varphi}(\alpha, \delta) = \int_0^\infty \int_0^\infty \varphi(\alpha, \delta) \pi_\rho(\alpha, \delta | \underline{X}) d\alpha d\delta.$$

It is clear that from Equation (11), the marginal PDFs of  $\alpha$  and  $\delta$  cannot be obtained in explicit expression. For this purpose, we propose using Bayes Monte Carlo Markov chain (MCMC) techniques to generate samples from Equation (11) in order to compute the acquired Bayes estimates and to construct their HPD intervals.

To run the MCMC sampler, from Equation (11), the full conditional PDFs of  $\alpha$  and  $\delta$  are given, respectively, as

$$\pi_\rho^\alpha(\alpha | \delta, \underline{X}) \propto \alpha^{D_\rho+a_1-1} e^{1-\alpha b_1 - (\psi(\delta; x_j))^\alpha} \Psi_\rho(T_\tau; \alpha, \delta) \prod_{j=1}^{D_\rho} (\psi(\delta; x_j))^\alpha [1 - e^{1-(\psi(\delta; x_j))^\alpha}]^{R_j}, \quad (12)$$

and

$$\pi_\rho^\delta(\delta | \alpha, \underline{X}) \propto \delta^{D_\rho+a_2-1} e^{1-\delta b_2 - (\psi(\delta; x_j))^\alpha} \Psi_\rho(T_\tau; \alpha, \delta) \prod_{j=1}^{D_\rho} (\psi(\delta; x_j))^{\alpha-1} [1 - e^{1-(\psi(\delta; x_j))^\alpha}]^{R_j}, \quad (13)$$

Since the posterior PDFs of  $\alpha$  and  $\delta$  in Equations (12) and (13), respectively, cannot be reduced analytically to any familiar distribution, the Metropolis–Hastings (M-H) algorithm is considered to solve this problem (for detail, see Gelman et al. [19] and Lynch [20]). The sampling process of the M-H algorithm is conducted as follows:

**Step 1:** Set the initial values  $\alpha^{(0)} = \hat{\alpha}$  and  $\delta^{(0)} = \hat{\delta}$ .

**Step 2:** Set  $S = 1$ .

**Step 3:** Generate  $\alpha^*$  and  $\delta^*$  from  $N(\hat{\alpha}, \hat{\sigma}_{11})$  and  $N(\hat{\delta}, \hat{\sigma}_{22})$ , respectively.

**Step 4:** Obtain  $\zeta_\alpha = \min \left\{ 1, \frac{\pi_\alpha^\alpha(\alpha^* | \delta^{(S-1)}, \underline{X})}{\pi_\alpha^\alpha(\alpha^{(S-1)} | \delta^{(S-1)}, \underline{X})} \right\}$  and  $\zeta_\delta = \min \left\{ 1, \frac{\pi_\delta^\delta(\delta^* | \alpha^{(S)}, \underline{X})}{\pi_\delta^\delta(\delta^{(S-1)} | \alpha^{(S)}, \underline{X})} \right\}$ .

**Step 5:** Generate samples  $u_1$  and  $u_2$  from the uniform  $U(0, 1)$  distribution.

**Step 6:** If  $u_1 \leq \zeta_\alpha$  and  $u_2 \leq \zeta_\delta$ , then set  $\alpha^{(S)} = \alpha^*$  and  $\delta^{(S)} = \delta^*$ ; otherwise, set  $\alpha^{(S)} = \alpha^{(S-1)}$  and  $\delta^{(S)} = \delta^{(S-1)}$ , respectively.

**Step 7:** Set  $S = S + 1$ .

**Step 8:** Repeat steps 3–7  $B$  times and obtain  $\alpha^{(S)}$  and  $\delta^{(S)}$  for  $S = 1, 2, \dots, B$ .

**Step 9:** Compute the RF (Equation (4)) and HF (Equation (5)) using  $(\alpha^{(S)}, \delta^{(S)})$ ,  $S = 1, 2, \dots, B$  for a given mission time  $t > 0$ , respectively, as

$$R^{(S)}(t) = 1 - \exp \left( 1 - \left( 1 + \delta^{(S)} t^{-1} \right)^{\alpha^{(S)}} \right),$$

and

$$h^{(S)}(t) = \frac{\alpha^{(S)} \delta^{(S)} t^{-2} \left( 1 + \delta^{(S)} t^{-1} \right)^{\alpha^{(S)} - 1}}{\exp \left( \left( 1 + \delta^{(S)} t^{-1} \right)^{\alpha^{(S)}} - 1 \right) - 1}.$$

To guarantee the convergence of the MCMC sampler and remove the affection of the start values  $\alpha^{(0)}$  and  $\delta^{(0)}$ , the first simulated varieties (say  $B_0$ ) are discarded as burn-ins. Therefore, the remaining  $B - B_0$  samples of  $\alpha$ ,  $\delta$ ,  $R(t)$  or  $h(t)$  (say  $\varphi$ ) are utilized to compute the Bayesian estimates. However, the Bayes MCMC estimates of  $\varphi$  under the SE loss function are given by

$$\tilde{\varphi} = \frac{1}{B - B_0} \sum_{S=B_0+1}^B \varphi^{(S)}.$$

#### 4. Interval Estimators

In this section, the approximate confidence (based on the observed Fisher information) and HPD interval (based on the MCMC-simulated varieties) estimators of  $\alpha$ ,  $\delta$ ,  $R(t)$ , or  $h(t)$  are obtained.

##### 4.1. Asymptotic Intervals

To construct the ACIs for  $\alpha$  and  $\delta$ , we first need to compute the asymptotic variance-covariance (AVC) matrix, which is obtained by inverting the Fisher information matrix. Under some regularity conditions,  $(\hat{\alpha}, \hat{\delta})$  is approximately normal with a mean  $(\alpha, \delta)$  and variance  $\mathbf{I}^{-1}(\alpha, \delta)$ . Following Lawless [21], by setting  $\hat{\alpha}$  and  $\hat{\delta}$  in place of  $\alpha$  and  $\delta$ , we estimate  $\mathbf{I}^{-1}(\alpha, \delta)$  by  $\mathbf{I}^{-1}(\hat{\alpha}, \hat{\delta})$  as follows:

$$\mathbf{I}^{-1}(\hat{\varphi}) \cong \begin{bmatrix} -\mathcal{I}_{11} & -\mathcal{I}_{12} \\ -\mathcal{I}_{21} & -\mathcal{I}_{22} \end{bmatrix}^{-1} = \begin{bmatrix} \hat{\sigma}_{11} & \hat{\sigma}_{12} \\ \hat{\sigma}_{21} & \hat{\sigma}_{22} \end{bmatrix}, \quad (14)$$

where  $\hat{\varphi} = (\hat{\alpha}, \hat{\delta})^T$  and  $\mathcal{I}_{ij}$ ,  $i, j = 1, 2$  are obtained and reported in Appendix A. Thus, the two-sided  $100(1 - q)\%$  ACIs for  $\alpha$  and  $\delta$  are given, respectively, by

$$\left( \hat{\alpha} \pm z_{q/2} \sqrt{\hat{\sigma}_{11}} \right) \quad \text{and} \quad \left( \hat{\delta} \pm z_{q/2} \sqrt{\hat{\sigma}_{22}} \right),$$

where  $z_{q/2}$  denotes the upper  $q/2$  percentage points of the standard normal distribution, where  $\hat{\sigma}_{11}$  and  $\hat{\sigma}_{22}$  are the main diagonal elements of Equation (14).

Moreover, to construct the ACIs of  $R(t)$  and  $h(t)$ , we first follow the delta method to find the estimated variance of  $\hat{R}(t)$  and  $\hat{h}(t)$  (see Greene [22]) as follows:

$$\hat{\sigma}_{\hat{R}(t)}^2 = \mathbf{Y}_{\hat{R}}^T \mathbf{I}^{-1}(\hat{\varphi}) \mathbf{Y}_{\hat{R}} \quad \text{and} \quad \hat{\sigma}_{\hat{h}(t)}^2 = \mathbf{Y}_{\hat{h}}^T \mathbf{I}^{-1}(\hat{\varphi}) \mathbf{Y}_{\hat{h}},$$

where  $\mathbf{Y}_{\hat{R}}^T = \left[ \frac{\partial R(t)}{\partial \alpha}, \frac{\partial R(t)}{\partial \delta} \right]_{(\hat{\alpha}, \hat{\delta})}$  and  $\mathbf{Y}_{\hat{h}}^T = \left[ \frac{\partial h(t)}{\partial \alpha}, \frac{\partial h(t)}{\partial \delta} \right]_{(\hat{\alpha}, \hat{\delta})}$ .

Then, the two-sided  $100(1 - q)\%$  ACIs of  $R(t)$  and  $h(t)$  are given, respectively, by

$$\left( \hat{R}(t) \pm z_{q/2} \sqrt{\sigma_{\hat{R}(t)}^2} \right) \quad \text{and} \quad \left( \hat{h}(t) \pm z_{q/2} \sqrt{\sigma_{\hat{h}(t)}^2} \right).$$

Bootstrapping techniques which improve estimators or build confidence intervals of  $\alpha$ ,  $\delta$ ,  $R(t)$ , or  $h(t)$  can be easily incorporated.

#### 4.2. HPD Intervals

To construct  $100(1 - q)\%$  HPD interval estimates of  $\alpha$ ,  $\delta$ ,  $R(t)$ , or  $h(t)$ , the method suggested by Chen and Shao [23] is used. First, we order the MCMC samples of  $\varphi^{(j)}$  for  $j = B_0 + 1, B_0 + 2, \dots, B$  as  $\varphi_{(B_0+1)}, \varphi_{(B_0+2)}, \dots, \varphi_{(B)}$ . As a result, the  $100(1 - q)\%$  two-sided HPD interval of  $\varphi$  is given by

$$\left( \varphi_{(j^*)}, \varphi_{(j^* + (1-q)(B-B_0))} \right),$$

where  $j^* = B_0 + 1, B_0 + 2, \dots, B$  is chosen such that

$$\varphi_{(j^* + (1-q)(B-B_0))} - \varphi_{(j^*)} = \min_{1 \leq j \leq q(B-B_0)} \left( \varphi_{(j + (1-q)(B-B_0))} - \varphi_{(j)} \right),$$

here  $[x]$  denotes the highest value less than or equal to  $x$ .

### 5. Monte Carlo Simulation

To examine the performance of the proposed point and interval estimators introduced in the previous sections, an extensive Monte Carlo simulation is conducted. A total of 2000 GPHCS-T2 samples are generated from INH(0.5, 0.5) based on different choices for  $n$  (total test units),  $r$  (observed failure data),  $T_1, T_2$  (ideal times), and  $\underline{R}$  (censoring plan). At mission time  $t = 0.1$ , the actual values of  $R(t)$  and  $h(t)$  are 0.765 and 3.13, respectively. To run the experiment according to generalized progressive Type-II hybrid censored sampling from the proposed model, we propose the following algorithm:

**Step 1.** Set the parameter values of  $\alpha$  and  $\delta$ .

**Step 2.** Set the specific values of  $n, r, T_1, T_2$ , and  $\underline{R}$ .

**Step 3.** Simulate a PCS-T2 sample of size  $r$  as follows:

- Generate  $\nu$  independent observations of a size  $r$  as  $\nu_1, \nu_2, \dots, \nu_r$  from  $U(0, 1)$ .
- Set  $\omega_i = \nu_i \left( i + \sum_{j=r-i+1}^r R_j \right)^{-1}$ ,  $i = 1, 2, \dots, r$ .
- Set  $U_i = 1 - \omega_r \omega_{r-1} \cdots \omega_{r-i+1}$  for  $i = 1, 2, \dots, r$ .
- Carry out the PCS-T2 sample of a size  $r$  from INH( $\alpha, \delta$ ) by inverting Equation (3) (i.e.,  $X_i = F^{-1}(u_i; \alpha, \delta)$ ,  $i = 1, 2, \dots, r$ ).

**Step 4.** Determine  $d_1$  at  $T_1$  and  $d_2$  at  $T_2$  from the PCS-T2 sample.

**Step 5.** Carry out the GPHCS-T2 sample as follows:

- If  $X_r < T_1$ , then set  $R_i = 0$ , for  $i = r, r + 1, \dots, d_1$ , terminate the experiment at  $T_1$ , and remove the remaining units  $n - d_1 - \sum_{i=1}^{r-1} R_i$ . This is Case-I, and

- in this case, replace  $X_i, i = r, \dots, d_1$  with those items obtained from a truncated distribution  $f(x)[1 - F(x_r)]^{-1}$  with a size  $n - r - \sum_{i=1}^{r-1} R_i$ .
- b. If  $T_1 < X_r < T_2$ , then terminate the experiment at  $X_r$  and remove the remaining units  $n - r - \sum_{i=1}^{r-1} R_i$ . This is Case-II.
  - c. If  $T_1 < T_2 < X_r$ , then terminate the experiment at  $T_2$  and remove the remaining units  $n - d_2 - \sum_{i=1}^{d_2} R_i$ . This is Case-III.

For the given times  $(T_1, T_2) = (0.2, 0.4)$  and  $(0.4, 0.8)$ , various choices of  $n$  and  $r$  are also considered, such as  $n = (40, 80)$ , and  $r$  is taken as the failure percentage (FP) such that  $r/n = (50, 75, 100)\%$  for each  $n$ . For each given set of  $(n, r)$ , seven different PCSs  $S_i = (R_1, R_2, \dots, R_r), i = 1, 2, \dots, 7$ , where  $R = (4, 0, 0, 0, 4)$ , denoted by  $R = (4, 0^*3, 4)$ , are considered (see Table 2). Two different sets of the hyperparameters  $a_i, b_i, i = 1, 2$ , are used, namely  $(a_i, b_i) = (1, 2), i = 1, 2$  (prior A) and  $(a_i, b_i) = (5, 10), i = 1, 2$  (prior B). The specified values for priors A and B are determined in such a way that the prior average returns to the true value of the target parameter.

**Table 2.** Various PCSs used in Monte Carlo simulation.

$n$	Scheme	FPs		
		50%	75%	100%
40	S1	(1*20)	(1*10, 0*20)	(0*40)
	S2	(2*10, 0*10)	(0*20, 1*10)	-
	S3	(0*10, 2*10)	(2*5, 0*25)	-
	S4	(0*8, 4*5, 0*7)	(0*25, 2*5)	-
	S5	(0*5, 2*10, 0*5)	(0*13, 2*5, 0*12)	-
	S6	(2*5, 0*10, 2*5)	(0*10, 1*10, 0*10)	-
	S7	(0*19, 20)	(0*29, 10)	-
80	S1	(1*40)	(1*20, 0*40)	(0*80)
	S2	(2*20, 0*20)	(0*40, 1*20)	-
	S3	(0*20, 2*20)	(2*10, 0*50)	-
	S4	(0*16, 4*10, 0*14)	(0*50, 2*10)	-
	S5	(0*10, 2*20, 0*10)	(0*26, 2*10, 0*24)	-
	S6	(2*10, 0*20, 2*10)	(0*20, 1*20, 0*20)	-
	S7	(0*39, 40)	(0*59, 20)	-

For each unknown parameter, via the M-H sampler, 12,000 MCMC variates are generated, and the first 2000 values are eliminated as burn-ins. Hence, using the last 10,000 MCMC samples, the average Bayes estimates and 95% two-sided HPD intervals are computed. To run the MCMC sampler, the initial values of  $\alpha$  and  $\delta$  are taken to be  $\hat{\alpha}$  and  $\hat{\delta}$ , respectively.

A comparison between different point estimates is made based on their RMSE and MRAB values. Additionally, the performances of the proposed interval estimates are compared by using their ACLs. For the unknown parameter  $\alpha, \delta, R(t)$ , or  $h(t)$  (say  $\varphi_s, s = 1, 2, 3, 4$ ), the average estimates (Av.Es), RMSEs, MRABs and ACLs of  $\varphi_s$  are computed as follows:

$$\overline{\hat{\varphi}}_s = \frac{1}{N} \sum_{j=1}^N \hat{\varphi}_s^{(j)},$$

$$RMSE(\hat{\varphi}_s) = \sqrt{\frac{1}{N} \sum_{j=1}^N (\hat{\varphi}_s^{(j)} - \varphi_s)^2},$$

$$MRAB(\hat{\varphi}_s) = \frac{1}{N} \sum_{j=1}^N \frac{|\hat{\varphi}_s^{(j)} - \varphi_s|}{\varphi_s},$$

and

$$ACL_{\varphi_s}(1 - q)\% = \frac{1}{N} \sum_{j=1}^N (\mathcal{U}(\hat{\varphi}_s^{(j)}) - \mathcal{L}(\hat{\varphi}_s^{(j)})),$$



where  $\hat{\varphi}_s^{(j)}$  denotes the calculated estimate at the  $j$ th sample of  $\varphi_s$ ,  $\mathcal{N}$  is the number of generated sequence data, and  $\mathcal{L}(\cdot)$  and  $\mathcal{U}(\cdot)$  denote the lower and upper bounds, respectively, of the  $(1 - q)\%$  asymptotic (or credible HPD) interval of  $\varphi_s$  such that  $\varphi_1 = \alpha$ ,  $\varphi_2 = \delta$ ,  $\varphi_3 = R(t)$  and  $\varphi_4 = h(t)$ . All numerical computations were performed via the ‘maxLik’ and ‘coda’ packages in R 4.0.4 software.

Graphically, utilizing heat-map plots, all simulated values for the RMSEs, MRABs, and ACLs of  $\alpha$ ,  $\delta$ ,  $R(t)$ , and  $h(t)$  are shown in Figures 2–5, respectively, while all simulation tables are provided as Supplementary Materials.

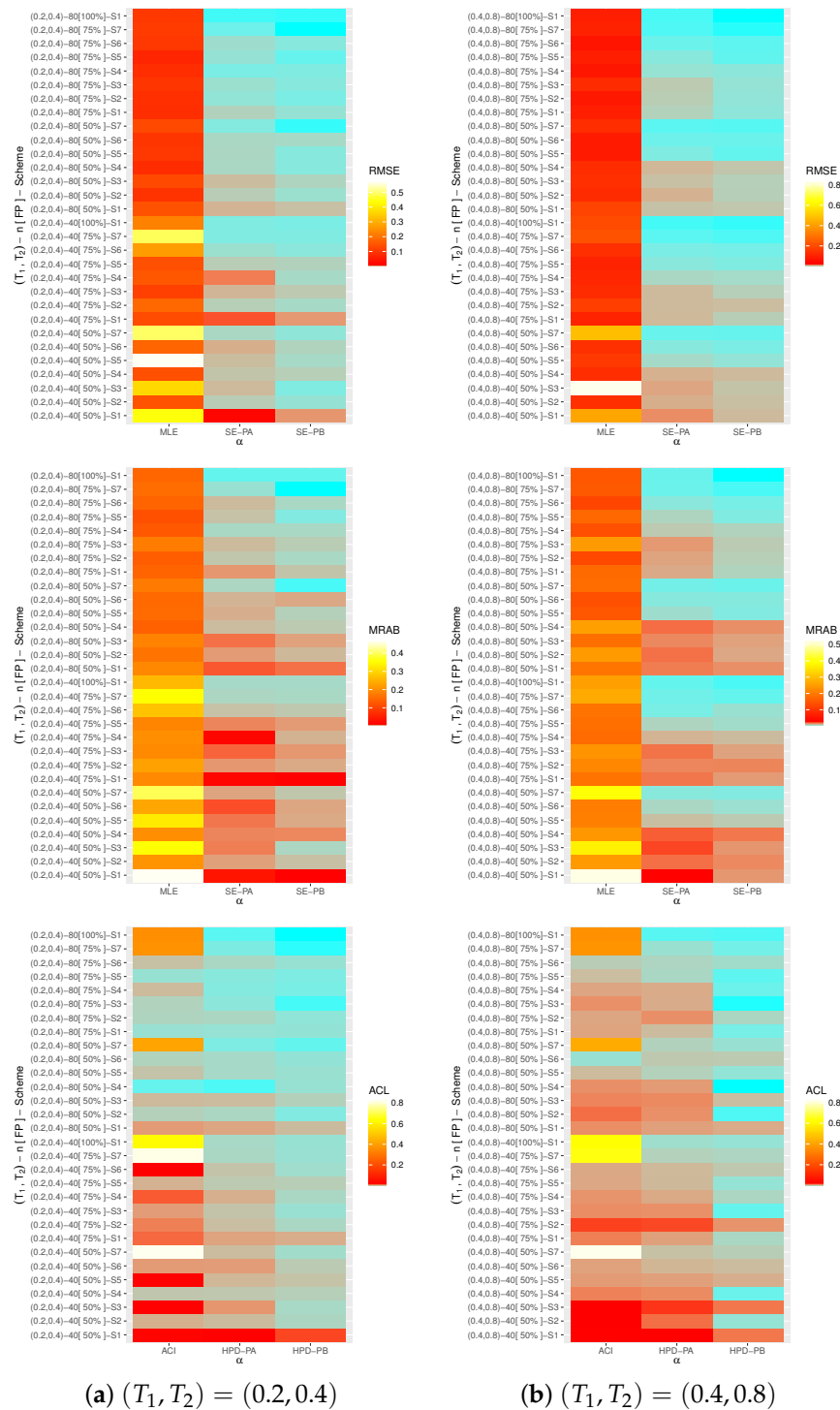


Figure 2. Heat-maps for the estimation results for  $\alpha$ .

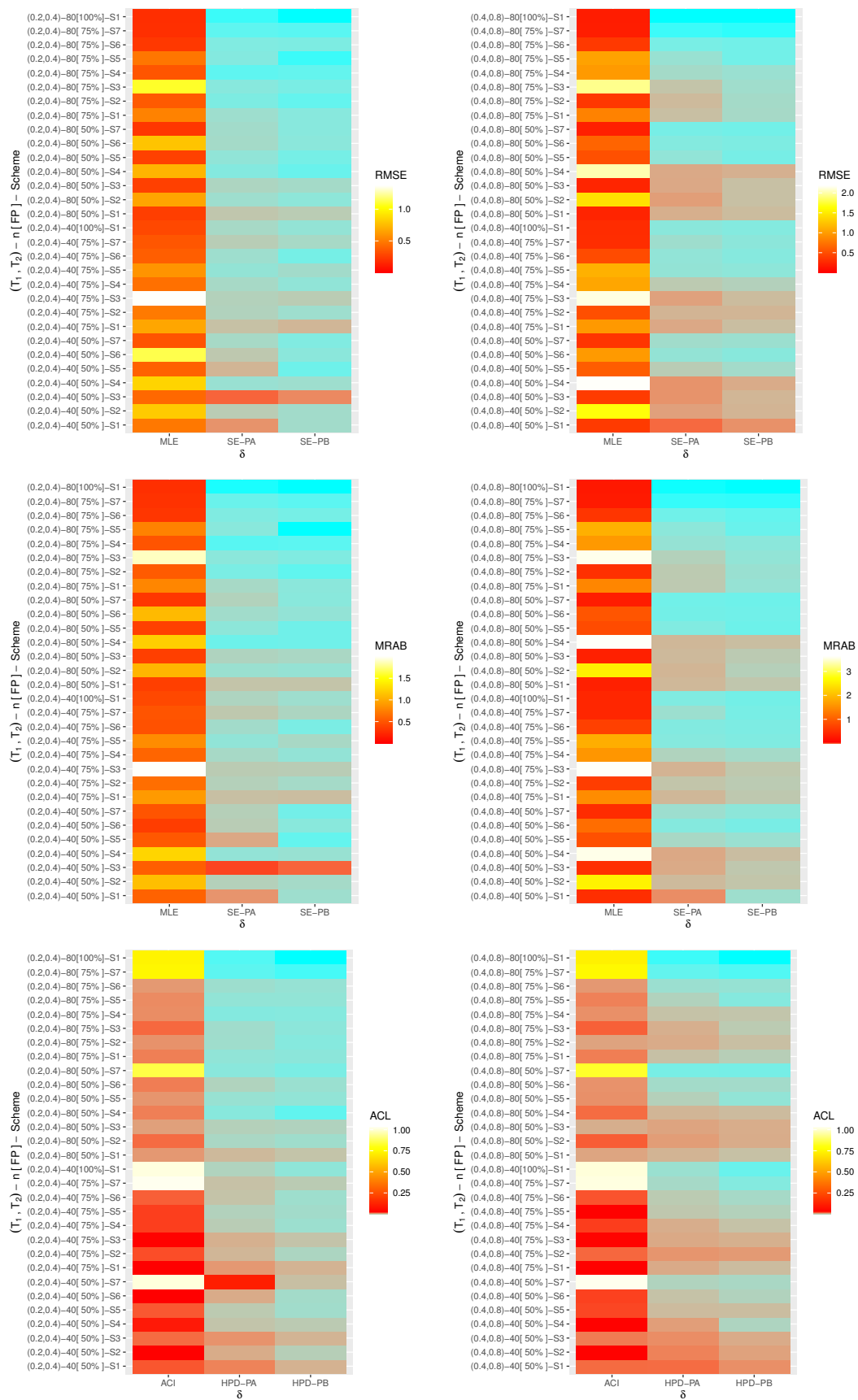


Figure 3. Heat-maps for the estimation results for  $\delta$ .

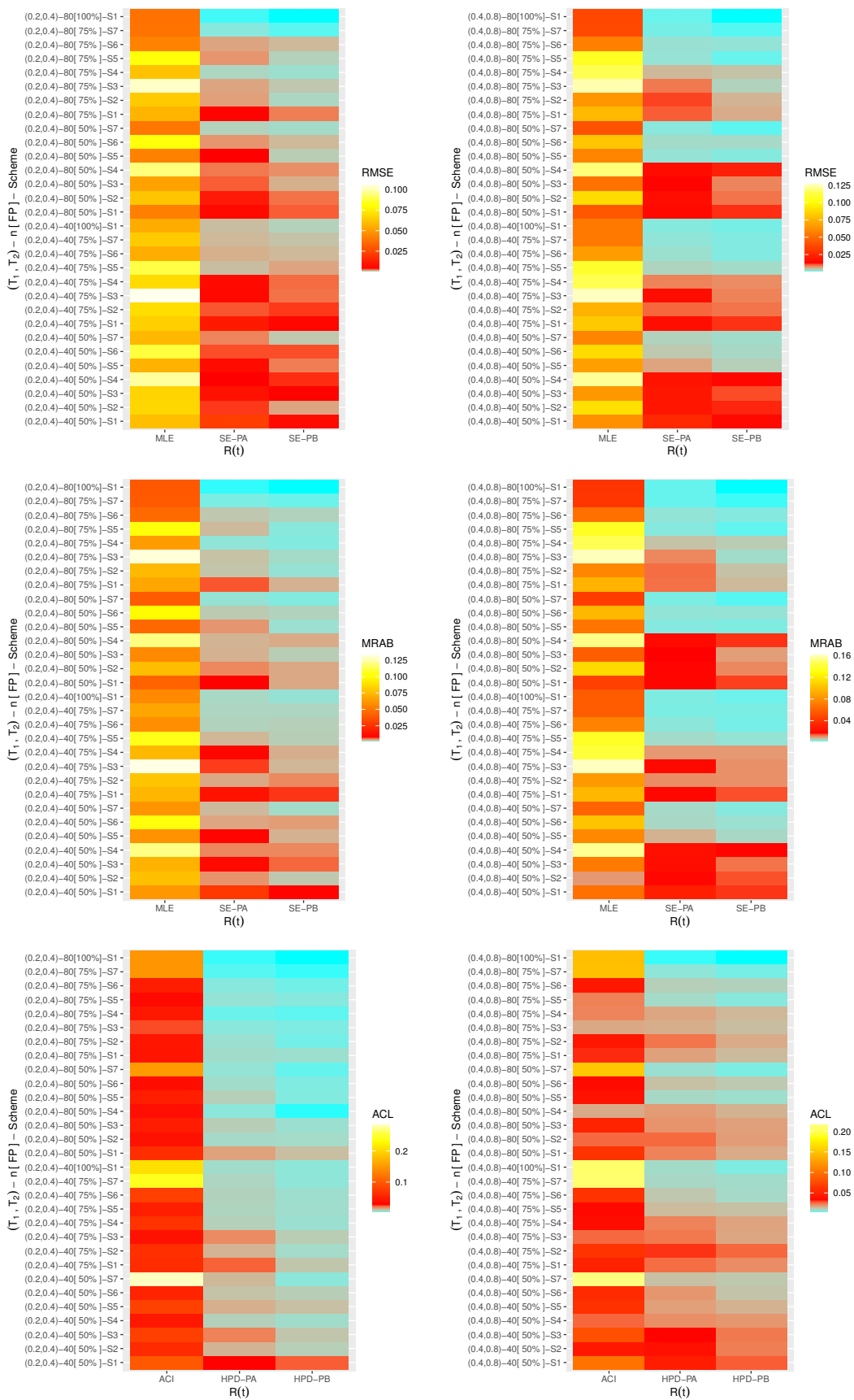
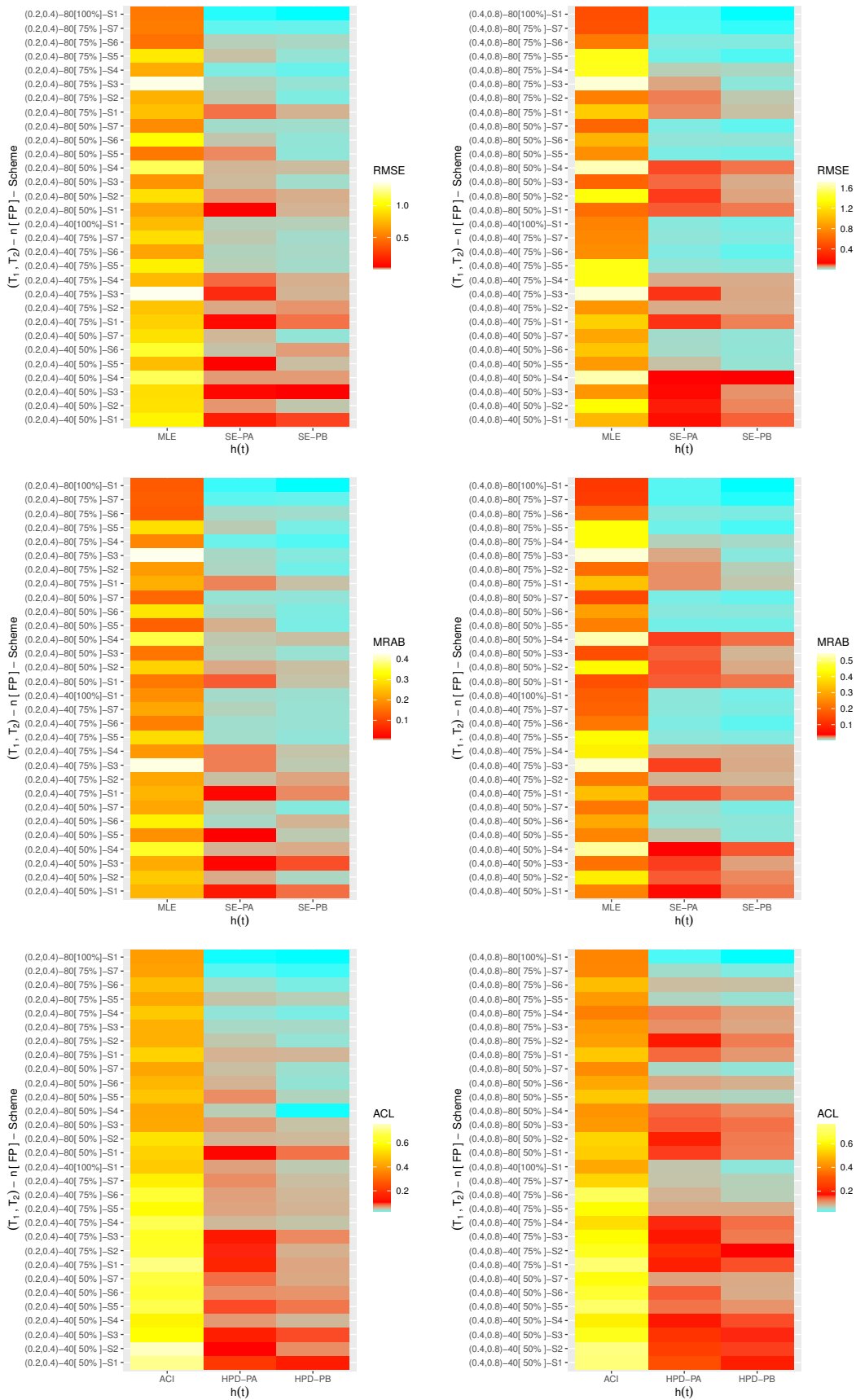


Figure 4. Heat-maps for the estimation results for  $R(t)$ .



(a)  $(T_1, T_2) = (0.2, 0.4)$

(b)  $(T_1, T_2) = (0.4, 0.8)$

Figure 5. Heat-maps for the estimation results for  $h(t)$ .

For specification, for each plot in Figures 2–5, some notations have been used. For example, based on prior A (PA), for all unknown parameters, the Bayes estimates based on the SE loss function are mentioned as ‘SE-PA’, and their HPD interval estimates are mentioned as ‘HPD-PA’. From Figures 2–5, some general observations can be made:

- The Bayesian estimates of all unknown parameters performed better than the frequentist estimates, as expected, in terms of the minimum RMSE, MRAB, and ACL values. This result was due to the fact that the Bayes point (or interval) estimates contained priority information of the model parameters but the others did not.
- As  $n$  (or FP) increases, the RMSEs, MRABs, and ACLs of all proposed estimates performed satisfactory. Similar performance was also observed when the sum of the removal patterns  $R_i$ ,  $i = 1, 2, \dots, r$  decreased.
- As  $T_i$ ,  $i = 1, 2$  increased, in most cases, the RMSEs and MRABs of all calculated estimates decreased significantly.
- As  $T_i$ ,  $i = 1, 2$ , tended to increase, the ACLs for ACIs of  $\alpha$  and  $R(t)$  decreased while the HPD intervals increased. In addition, the ACLs of the ACI and HPD intervals for  $\delta$  and  $h(t)$  narrowed.
- Since the variance of prior B was lower than the variance of prior A, the Bayesian results, including the point and interval estimators of  $\alpha$ ,  $\delta$ ,  $R(t)$ , and  $h(t)$ , performed better under prior B than those obtained under prior A in terms of their RMSEs, MRABs, and ACLs.
- To sum up, the simulation results recommended that the Bayesian inferential approach via the M-H algorithm was the better than the others for estimating the unknown parameter(s) of life using generalized Type-II progressive hybrid censored data.

## 6. Optimal PCS-T2 Plans

Mostly in the context of reliability, the experimenter may desire to determine the ‘best’ censoring scheme from a collection of all available censoring schemes in order to provide the most information about the unknown parameters under study. Balakrishnan and Aggarwala [24] first investigated the problem of choosing the optimal censoring strategy in various scenarios. Many optimality criteria, however, have been proposed, and numerous results on optimal censoring designs have been investigated. The specific values of  $n$  (total test units),  $r$  (effective sample), and  $T_i$ ,  $i = 1, 2$  (ideal test thresholds) are chosen in advance based on the availability of the units, experimental facilities, and cost considerations, as well as the optimal censoring design  $\underline{R} = (R_1, R_2, \dots, R_r)$ , where  $\sum_{i=1}^r R_i = n - r$ , can be determined (see Ng et al. [25]). In the literature, several works have addressed the problem of comparing two (or more) different censoring plans (for example, see Pradhan and Kundu [26], Elshahhat and Rastogi [16], Elshahhat and Abu El Azm [27], and Ashour et al. [28]). However, to determine an optimum PCS-T2 plan, some commonly-used criteria were considered (see Table 3).

**Table 3.** Some optimality criteria of progressive censoring plan.

Criterion	Objective
$C_1$	Minimize $\det(\mathbf{I}^{-1}(\hat{\phi}))$
$C_2$	Minimize $\text{trace}(\mathbf{I}^{-1}(\hat{\phi}))$
$C_3$	Maximize $\text{trace}(\mathbf{I}(\hat{\phi}))$
$C_4$	Minimize $\text{Var}(\log(\hat{T}_v))$
$C_5$	Minimize $\int_0^1 \text{Var}(\log(\hat{T}_v))w(v)dv$

From Table 3, it should be noted that the criteria  $C_1$  and  $C_2$  are intended to minimize the determinant and trace of the AVC matrix in Equation (14), while the criterion  $C_3$  is intended to maximize the main diagonal elements of the observed Fisher’s matrix  $\mathbf{I}(\alpha, \delta)$  at its MLEs  $\hat{\alpha}$  and  $\hat{\delta}$ . Regarding criteria  $C_1$  and  $C_2$ , Gupta and Kundu [29] stated that the comparison of two (or more) AVC matrices based on these criteria is not a trivial task because they are not scale-invariant.

Thus, based on criteria  $C_4$  and  $C_5$ , which are scale-invariant, one can determine the optimum censoring scheme of multi-parameter distributions. It is clear that the minimizing the associated variance of the logarithmic  $v$ th quantile  $\log(\hat{\mathcal{T}}_v)$ , where  $0 < v < 1$ , is dependent on the choice of  $v$  in  $C_4$ . Additionally, for  $C_5$ , the weight  $w(v) \geq 0$  is a nonnegative function satisfying  $\int_0^1 w(v)dv = 1$ . Hence, the logarithmic for  $\mathcal{T}_v$  of the INH distribution is

$$\log(\mathcal{T}_v) = \log(\delta) - \log((1 - \log(v))^{1/\alpha} - 1), \quad 0 < v < 1. \quad (15)$$

Again, using Equation (15), the delta method is considered here to approximate the variance estimate of  $\log(\hat{\mathcal{T}}_p)$  (say  $\widehat{var}(\log(\hat{\mathcal{T}}_p))$ ), as follows:

$$\widehat{var}(\log(\hat{\mathcal{T}}_p)) = \mathbf{Y}_{\log(\hat{\mathcal{T}}_p)}^T \mathbf{I}^{-1}(\hat{\phi}) \mathbf{Y}_{\log(\hat{\mathcal{T}}_p)},$$

where

$$\mathbf{Y}_{\log(\hat{\mathcal{T}}_p)}^T = \left[ \frac{\partial}{\partial \alpha} \log(\mathcal{T}_p), \frac{\partial}{\partial \delta} \log(\mathcal{T}_p) \right]_{(\hat{\alpha}, \hat{\delta})}$$

is the gradient of  $\log(\hat{\mathcal{T}}_p)$  with respect to  $\alpha$  and  $\delta$ . Obviously, from Table 3, it can be seen that the optimized PCS-T2 plan that provides more information corresponded to the smallest value of  $C_i$ ,  $i = 1, 2, 4, 5$  optimality criteria and the highest value of  $C_4$  optimality criteria.

## 7. Real-Life Applications

To demonstrate the adaptability and flexibility of the proposed methodologies to a real phenomenon, in this section, we shall provide two numerical applications using electronic devices and COVID-19 data sets.

### 7.1. Electronic Device Data

In this application, we'll analyze engineering real data given by Wang [30]. This data set consists of 18 observations of failure times of electronic devices: 5, 11, 21, 31, 46, 75, 98, 122, 145, 165, 196, 224, 245, 293, 321, 330, 350, and 420. We first checked whether Wang's data fit INH distribution or not. For this purpose, the Kolmogorov–Smirnov (K-S) distance along with the associated  $p$ -value provided. Using all of Wang's data, the MLEs (with their standard errors (St.E)) of  $\alpha$  and  $\delta$  were 0.4215 (0.1073) and 258.03 (164.65), respectively, and the K-S (with its  $p$ -value) was 0.199 (0.418). This result indicates that Wang's data were coming from INH lifetime model. To show the existence and uniqueness of  $\hat{\alpha}$  and  $\hat{\delta}$ , the contour plot of the log-likelihood function with respect to  $\alpha$  and  $\delta$  using all of Wang's data is plotted in Figure 6a. It shows that the MLEs  $\hat{\alpha} \cong 0.42$  and  $\hat{\delta} \cong 258.03$  existed and were unique. It is also clear that Wang's data set was overly and generally flat. We also suggest taking these estimates as initial values to run any numerical evaluation required. Graphically, to identify the HF shapes of Wang's data, the scaled total time on testing (TTT) transform is also plotted in Figure 6b. It indicates that the bathtub-shaped (decreasing-increasing) hazard rate was suitable for the fitting the INH model.

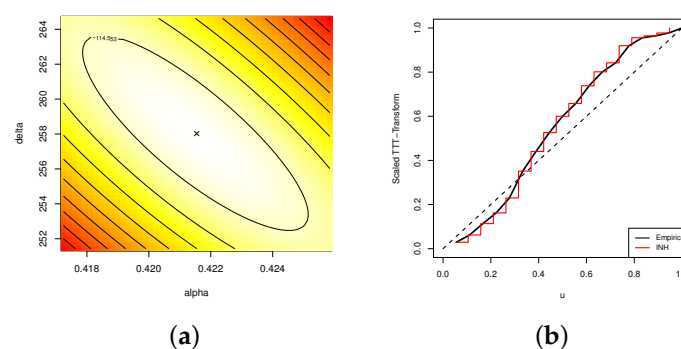


**Figure 6.** (a) Contour plot of log-likelihood function and (b) empirical and fitted scaled TTT transform plot from Wang's data.

From all of Wang’s data, based on various choices of  $T_i$ ,  $i = 1, 2$  and different PCSs  $\underline{R}$ , namely  $S_1: \underline{R} = (1^*9)$ ,  $S_2: \underline{R} = (2^*4, 0^*4, 1)$ , and  $S_3: \underline{R} = (1, 0^*4, 2^*4)$ , different artificial GPHCS-T2 samples were generated when  $r = 9$ , which are presented in Table 4. Since the prior information about the model parameters was not available, the improper gamma priors (i.e.,  $a_i = b_i = 0$ , for  $i = 1, 2$ ) were used. However, to run the calculations, we used 0.0001 for all given hyperparameters. Using the MCMC algorithm described in Section 3, to develop the Bayes point estimates and associated HPD interval estimates, the first 5000 iterations were discarded from 30,000 MCMC samples. From Table 4, it can be seen that the point (with their St.Es) and 95% interval (with their interval lengths (ILs)) estimators derived by the maximum likelihood and Bayesian approaches of  $\alpha$ ,  $\delta$ ,  $R(t)$ , and  $h(t)$  (at time  $t = 50$ ) were computed, and they are presented in Table 5. It is evident that the acquired inferences of  $\alpha$ ,  $\delta$ ,  $R(t)$ , and  $h(t)$  derived using the Bayes approach performed better than those derived from the frequentist approach in terms of their minimum St.E and IL values.

**Table 4.** Three artificial GPHCS-T2 samples from Wang’s data.

Scheme	Sample	$T_1(d_1)$	$T_2(d_2)$	Censored Data	R*	T*
$S_1$	1	450 (10)	500 (10)	5, 21, 46, 98, 145, 196, 245, 321, 350, 420	1	450
	2	450 (9)	500 (9)	5, 21, 46, 98, 145, 196, 245, 321, 350	0	350
	3	200 (6)	340 (8)	5, 21, 46, 98, 145, 196, 245, 321	2	340
$S_2$	1	450 (10)	500 (10)	5, 31, 98, 165, 245, 293, 321, 330, 350, 420	1	450
	2	300 (6)	500 (9)	5, 31, 98, 165, 245, 293, 321, 330, 350	0	350
	3	250 (5)	340 (8)	5, 31, 98, 165, 245, 293, 321, 330	2	340
$S_3$	1	400 (10)	450 (11)	5, 21, 31, 46, 75, 98, 165, 245, 330, 350	1	400
	2	150 (6)	450 (9)	5, 21, 31, 46, 75, 98, 165, 245, 330	0	330
	3	100 (6)	325 (8)	5, 21, 31, 46, 75, 98, 165, 245	3	325

**Table 5.** The point and interval estimates of  $\alpha$ ,  $\delta$ ,  $R(t)$ , and  $h(t)$  under Wang’s data.

Scheme	Sample	Parameter	MLE		MCMC		ACI			HPD		
			Estimate	St.E	Estimate	St.E	Lower	Upper	IL	Lower	Upper	IL
$S_1$	1	$\alpha$	0.30525	0.04106	0.33224	0.04299	0.22477	0.38573	0.16096	0.27552	0.39430	0.11878
		$\delta$	1492.71	11.8654	1492.53	0.20787	1469.45	1515.96	46.5116	1492.33	1492.70	0.37533
		$R(50)$	0.84252	0.06315	0.87534	0.05439	0.71874	0.96630	0.24756	0.79636	0.94571	0.14935
	2	$h(50)$	0.00315	0.00063	0.00273	0.00066	0.00191	0.00438	0.00247	0.00178	0.00359	0.00181
		$\alpha$	0.32569	0.04731	0.29412	0.05086	0.23295	0.41842	0.18546	0.22589	0.37456	0.14867
		$\delta$	944.274	11.8656	944.027	0.25408	921.018	967.530	46.5125	943.913	944.140	0.22692
	3	$R(50)$	0.80756	0.07207	0.74986	0.09170	0.66630	0.94882	0.28253	0.62277	0.87664	0.25388
		$h(50)$	0.00390	0.00069	0.00432	0.00068	0.00255	0.00526	0.00271	0.00320	0.00522	0.00202
		$\alpha$	0.30451	0.04388	0.30628	0.03280	0.21851	0.39051	0.17200	0.25028	0.36237	0.11209
$S_2$	1	$\delta$	1258.83	8.38948	1258.84	0.04810	1242.39	1275.28	32.8861	1258.77	1258.93	0.16361
		$R(50)$	0.81778	0.07054	0.81586	0.05051	0.67953	0.95604	0.27651	0.71895	0.89717	0.17822
		$h(50)$	0.00353	0.00066	0.00349	0.00049	0.00224	0.00481	0.00257	0.00264	0.00429	0.00165
$S_3$	1	$\alpha$	0.32087	0.04271	0.33577	0.04173	0.23716	0.40457	0.16742	0.26254	0.41146	0.14892
		$\delta$	1508.79	8.38929	1508.80	0.05892	1492.35	1525.23	32.8854	1508.69	1508.88	0.18256
		$R(50)$	0.86671	0.05904	0.87944	0.04753	0.75100	0.98242	0.23142	0.80316	0.97292	0.16976
	2	$h(50)$	0.00288	0.00067	0.00265	0.00063	0.00158	0.00418	0.00261	0.00152	0.00376	0.00224
		$\alpha$	0.34508	0.05087	0.37573	0.07028	0.24537	0.44479	0.19941	0.26306	0.46711	0.20405
		$\delta$	863.796	11.8672	863.415	0.41156	840.536	887.055	46.5186	863.217	863.673	0.45605
	3	$R(50)$	0.82192	0.07172	0.84819	0.08310	0.68135	0.96249	0.28114	0.69969	0.95197	0.25228
		$h(50)$	0.00385	0.00075	0.00338	0.00105	0.00238	0.00532	0.00294	0.00204	0.00498	0.00294
		$\alpha$	0.32653	0.04783	0.33673	0.03512	0.23279	0.42027	0.18748	0.28515	0.39890	0.11376
$S_3$	1	$\delta$	1094.35	16.7840	1094.35	0.06937	1061.45	1127.24	65.7922	1094.22	1094.45	0.22733
		$R(50)$	0.83126	0.07019	0.84128	0.04651	0.69369	0.96884	0.27515	0.76761	0.92034	0.15273
		$h(50)$	0.00352	0.00072	0.00336	0.00053	0.00211	0.00494	0.00282	0.00243	0.00414	0.00171
	2	$\alpha$	0.29757	0.03992	0.29947	0.03588	0.21933	0.37580	0.15647	0.23477	0.35279	0.11803
		$\delta$	1394.83	6.34156	1394.92	0.10524	1382.40	1407.26	24.8585	1394.85	1394.98	0.13347
		$R(50)$	0.82108	0.06536	0.81815	0.06060	0.69298	0.94918	0.25619	0.70543	0.90181	0.19639
	3	$h(50)$	0.00341	0.00060	0.00336	0.00053	0.00223	0.00458	0.00236	0.00255	0.00429	0.00173
		$\alpha$	0.31500	0.04570	0.28327	0.04662	0.22543	0.40457	0.17915	0.20276	0.34460	0.14185
		$\delta$	918.421	10.6135	918.318	0.12350	897.619	939.223	41.6042	918.202	918.436	0.23408
$S_3$	2	$R(50)$	0.78637	0.07358	0.72742	0.08633	0.64217	0.93058	0.28842	0.61181	0.87589	0.26409
		$h(50)$	0.00413	0.00065	0.00454	0.00061	0.00285	0.00540	0.00255	0.00372	0.00550	0.00178
		$\alpha$	0.29328	0.04158	0.32213	0.04464	0.21177	0.37478	0.16301	0.26541	0.38712	0.12170
3	$\delta$	1258.08	23.7337	1257.90	0.20938	1211.56	1304.59	93.0344	1257.70	1258.07	0.37431	
	$R(50)$	0.79906	0.07103	0.83955	0.06405	0.65984	0.93829	0.27845	0.75083	0.92321	0.17237	
	$h(50)$	0.00370	0.00061	0.00325	0.00068	0.00250	0.00489	0.00239	0.00228	0.00411	0.00183	

According to the proposed criteria given in Table 3, the problem of determining the optimum progressive censoring plan is present. Using the generated samples in Table 4, the calculated values of the optimum criteria are presented in Table 6. To distinguish them, the suggested optimum censoring schemes are denoted with asterisks (\*). However, Table 6 shows that for Sample 1,  $S_1$  was the optimal censoring using  $C_3$ , and  $S_2$  was the optimal censoring using  $C_i, i = 4, 5$ , while  $S_3$  was the optimal censoring using  $C_i, i = 1, 2$ . For Samples 2 and 3,  $S_1$  was the optimal censoring using  $C_i, i = 1, 2, 3$ , while  $S_2$  was the optimal censoring using  $C_i, i = 4, 5$ .

**Table 6.** Optimum progressive censoring plan under Wang’s data.

Sample $v \rightarrow$	Scheme	$C_1$	$C_2$	$C_3$	$C_4$ $C_5$		
					0.3	0.6	0.9
1	$S_1$	0.23730	140.790	593.310 *	2082.197	16,339.83	367,978.2
	$S_2$	0.31504	140.796	446.917	1251.656 *	9004.943 *	196,306.7 *
	$S_3$	0.13547 *	70.3852 *	519.533	130.3598 *	1318.443 *	15,213.47 *
2	$S_1$	0.12835 *	70.3819 *	548.329 *	1682.934	13,251.48	298,739.9
	$S_2$	0.36422	140.833	386.670	167.2291	1871.671	22,894.99
	$S_3$	0.64385	281.706	437.535	2534.547	18,577.64	407,307.8
3	$S_1$	0.06406 *	40.2169 *	627.750 *	261.3108	2699.633	31,508.02
	$S_2$	0.23516	112.649	479.030	1335.744 *	8961.234 *	190,206.8 *
	$S_3$	0.97349	563.291	578.632	144.5508 *	1350.787 *	14,879.23 *
					1725.113	12,372.11	269,561.5
					179.9892	1813.738	20,893.35
					1630.251	13,276.49	303,198.9
					159.2986	1850.959	23,139.50
					1038.482 *	7803.217 *	172,917.4 *
					105.7014 *	1122.635 *	13,326.83 *
					1395.357	11,635.34	26,9434.4
					134.8670	1607.324	20,461.52

7.2. COVID-19 Data

This application provides an analysis of the confirmed deaths by the 7-day moving average for coronavirus disease (COVID-19) in the United States for 32 consecutive days from mid-March to mid-April 2020 (<https://www.cdc.gov/> accessed on 3 March 2022), see Table 7. To check for the goodness of fit, the K-S statistic along with the associated  $p$  value were obtained. First, using complete COVID-19 data, the MLEs (with their St.Es) of  $\alpha$  and  $\delta$  were 0.2989 (0.0521) and 1696.1 (895.34), respectively. Thus, the K-S (with its  $p$  value) was 0.1601 (0.348). This result demonstrates that the INH distribution is an adequate model to fit the COVID-19 data.

**Table 7.** Deaths due to COVID-19 from mid-March to mid-April 2020 in USA.

10	13	17	25	33	46	60	77
98	127	162	203	260	321	385	473
584	702	884	971	1120	1312	1448	1608
1763	1891	2009	2100	2102	2132	2188	2255

The contour plot, using the complete COVID-19 data set, of the log-likelihood function with respect to  $\alpha$  and  $\delta$  is displayed in Figure 7a. It indicates that the MLEs  $(\hat{\alpha}, \hat{\delta}) \cong (0.2989, 1696.1)$  existed and were unique. Additionally, a plot of the scaled TTT transform for the COVID-19 data is displayed in Figure 7b. It shows that the bathtub-shaped (decreasing-increasing) hazard rate was adequate for fitting the INH model.

In Table 8, from the complete COVID-19 data set when  $r = 12$ , different GPHCS-T2 samples based on various choices of  $T_i, i = 1, 2$ , and  $\underline{R}$  were generated, namely  $S_1: \underline{R} = (0, 2^*10, 0), S_2: \underline{R} = (4^*4, 0^*7, 4)$ , and  $S_3: \underline{R} = (4, 0^*7, 4^*4)$ . From Table 8, the maximum likelihood and Bayes estimates (with their St.Es) of  $\alpha, \delta, R(t)$ , and  $h(t)$  for time  $t = 100$  were computed, and they are presented in Table 9. In addition, two-sided 95% ACI and HPD intervals with their ILs were calculated, and these are also listed in Table 9. From Table 9, it can be seen that the calculated inferences derived from the Bayesian MCMC estimates in



terms of their St.Es performed better than the frequentist estimates, and the HPD interval estimates with respect to their ILs performed better than the others.

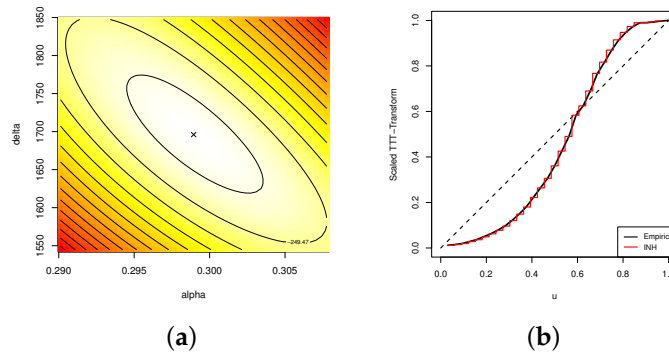


Figure 7. (a) Contour plot of log-likelihood function. (b) Empirical or fitted scaled TTT transform plot derived from COVID-19 data.

Table 8. Three GPHCS-T2 samples from COVID-19 data.

Scheme	Sample	$T_1(d_1)$	$T_2(d_2)$	Censored Data	$R^*$	$T^*$
$S_1$	1	2200 (13)	2300 (14)	10, 13, 33, 77, 162, 321, 584, 971, 1448, 1891, 2102, 2132, 2188	2	2100
	2	2000 (10)	2300 (14)	10, 13, 33, 77, 162, 321, 584, 971, 1448, 1891, 2102, 2255	0	2255
	3	1500 (9)	2200 (11)	10, 13, 33, 77, 162, 321, 584, 971, 1448, 1891, 2102	1	2200
$S_2$	1	2150 (14)	2300 (16)	10, 46, 162, 473, 1120, 1312, 1448, 1608, 1763, 1891, 2009, 2100, 2102, 2132	2	2150
	2	2000 (10)	2300 (16)	10, 46, 162, 473, 1120, 1312, 1448, 1608, 1763, 1891, 2009, 2100	0	2100
	3	1500 (7)	2000 (10)	10, 46, 162, 473, 1120, 1312, 1448, 1608, 1763, 1891	6	2000
$S_3$	1	2120 (13)	2300 (16)	10, 46, 60, 77, 98, 127, 162, 203, 260, 702, 1448, 2100, 2102	3	2120
	2	1500 (11)	2300 (16)	10, 46, 60, 77, 98, 127, 162, 203, 260, 702, 1448, 2100	0	2100
	3	750 (10)	1500 (11)	10, 46, 60, 77, 98, 127, 162, 203, 260, 702, 1448	6	1500

Table 9. The point and interval estimates of  $\alpha$ ,  $\delta$ ,  $R(t)$ , and  $h(t)$  under COVID-19 data.

Scheme	Sample	Parameter	MLE		MCMC		ACI			HPD		
			Estimate	St.E	Estimate	St.E	Lower	Upper	IL	Lower	Upper	IL
$S_1$	1	$\alpha$	0.24911	0.02608	0.23857	0.02787	0.19799	0.30023	0.10224	0.18368	0.28676	0.10308
		$\delta$	9934.79	11.86340	9934.54	0.26007	9911.54	9958.05	46.5037	9934.42	9934.66	0.23475
		$R(100)$	0.88376	0.04404	0.85936	0.05426	0.79744	0.97008	0.17263	0.76900	0.95615	0.18715
	2	$h(100)$	0.00102	0.00021	0.00111	0.00022	0.00061	0.00143	0.00082	0.00073	0.00152	0.00079
		$\alpha$	0.24880	0.02730	0.24886	0.02080	0.19529	0.30231	0.10702	0.21001	0.28791	0.07789
		$\delta$	8558.04	6.84928	8558.04	0.05323	8544.62	8571.47	26.8487	8557.97	8558.15	0.18334
	3	$R(100)$	0.86920	0.04834	0.86586	0.03675	0.77446	0.96393	0.18948	0.79577	0.93123	0.13546
		$h(100)$	0.00112	0.00022	0.00112	0.00016	0.00070	0.00155	0.00085	0.00081	0.00142	0.00061
		$\alpha$	0.24209	0.02660	0.24590	0.02654	0.18997	0.29422	0.10425	0.19570	0.30103	0.10533
$S_2$	1	$\delta$	9934.07	5.59244	9934.08	0.06100	9923.11	9945.03	21.9220	9933.97	9934.16	0.18831
		$R(100)$	0.87149	0.04807	0.87256	0.04356	0.77727	0.96570	0.18843	0.79971	0.96484	0.16513
		$h(100)$	0.00108	0.00021	0.00105	0.00021	0.00066	0.00149	0.00083	0.00061	0.00142	0.00081
	2	$\alpha$	0.30261	0.02899	0.31310	0.02675	0.24579	0.35944	0.11365	0.26374	0.35782	0.09408
		$\delta$	10195.0	4.84317	10194.8	0.21484	10185.5	10204.5	18.9849	10194.6	10195.0	0.37926
		$R(100)$	0.95334	0.02548	0.95839	0.02098	0.90339	0.99870	0.09531	0.91678	0.98954	0.07277
	3	$h(100)$	0.00060	0.00020	0.00054	0.00018	0.00020	0.00100	0.00080	0.00026	0.00087	0.00062
		$\alpha$	0.29585	0.03384	0.27814	0.03623	0.22952	0.36219	0.13267	0.21713	0.34464	0.12750
		$\delta$	6623.37	11.86333	6623.13	0.24825	6600.12	6646.62	46.5034	6623.02	6623.24	0.22556
$S_3$	1	$R(100)$	0.91566	0.04171	0.88500	0.05678	0.83391	0.99742	0.16351	0.80234	0.97176	0.16942
		$h(100)$	0.00093	0.00026	0.00107	0.00028	0.00041	0.00145	0.00104	0.00052	0.00148	0.00097
		$\alpha$	0.27929	0.03082	0.28023	0.02322	0.21888	0.33969	0.12080	0.23755	0.32289	0.08534
	2	$\delta$	9389.66	8.38862	9389.65	0.05237	9373.22	9406.10	32.8828	9389.58	9389.76	0.18064
		$R(100)$	0.92318	0.03844	0.92052	0.02836	0.84784	0.99852	0.15067	0.86550	0.96939	0.10389
		$h(100)$	0.00082	0.00024	0.00082	0.00018	0.00035	0.00129	0.00094	0.00050	0.00115	0.00065
	3	$\alpha$	0.24862	0.02464	0.25169	0.02476	0.20032	0.29691	0.09659	0.20520	0.30554	0.10034
		$\delta$	12501.5	7.50304	12501.5	0.06166	12486.8	12516.2	29.4114	12501.4	12501.6	0.18752
		$R(100)$	0.90252	0.03866	0.90216	0.03570	0.82675	0.97830	0.15155	0.84075	0.97538	0.13462
$S_3$	1	$h(100)$	0.00089	0.00020	0.00087	0.00019	0.00050	0.00127	0.00077	0.00043	0.00118	0.00076
		$\alpha$	0.24043	0.02691	0.24809	0.03211	0.18769	0.29316	0.10547	0.17909	0.29760	0.11851
		$\delta$	9970.42	8.38868	9970.02	0.43087	9953.98	9986.86	32.8830	9969.81	9970.29	0.47570
	2	$R(100)$	0.86880	0.04935	0.87421	0.05769	0.77208	0.96552	0.19344	0.74780	0.96061	0.21281
		$h(100)$	0.00109	0.00021	0.00103	0.00025	0.00067	0.00151	0.00084	0.00065	0.00155	0.00091
		$\alpha$	0.24267	0.02605	0.24884	0.01965	0.19162	0.29372	0.10211	0.21294	0.28306	0.07012
	3	$\delta$	10351.4	11.8632	10351.4	0.06944	10328.2	10374.7	46.5032	10351.3	10351.5	0.22800
		$R(100)$	0.87634	0.04628	0.88406	0.03206	0.78564	0.96705	0.18141	0.82553	0.94134	0.11582
		$h(100)$	0.00105	0.00021	0.00100	0.00016	0.00064	0.00146	0.00082	0.00073	0.00128	0.00055

To discuss how to select the optimum censoring plan from the COVID-19 data, based on the generated samples in Table 4, the calculated values of the given criteria  $S_i$ ,  $i = 1, 2, 3, 4, 5$  are reported in Table 10. It can be observed that for Sample 1,  $S_1$  was the optimal scheme under  $C_3$ , and  $S_2$  was the optimal scheme under  $C_i$ ,  $i = 4, 5$ , while  $S_3$  was the optimal scheme under  $C_i$ ,  $i = 1, 2$ . For Samples 2 and 3,  $S_1$  was the optimal scheme under  $C_i$ ,  $i = 1, 2, 3$ , while  $S_2$  was the optimal scheme under  $C_i$ ,  $i = 4, 5$  compared with the other competing schemes. As a result, great information about the unknown INH parameters could be easily obtained using two recommended censoring schemes, namely left withdrawn, where  $\underline{R} = (n - r, 0^*(r - 1))$ , and uniformly withdrawn, where  $\underline{R} = (1^*r)$ . This finding was due to the fact that the remaining surviving units were removed at an early stage (i.e.,  $R = (n - r, 0^*(r - 1))$  (left withdrawn) or  $R = (1^*r)$  (uniformly withdrawn)), and they could be used for other purposes, especially if the items put in the test were very costly. All conclusions derived from the COVID-19 data support the same findings in the case of electronic device data analysis. Finally, the analysis results from both the electronic devices and COVID-19 data sets support the simulation results.

**Table 10.** Optimum progressive censoring plan under COVID-19 data.

Sample	Scheme	$C_1$	$C_2$	$C_3$	$C_4$ $C_5$		
					0.3	0.6	0.9
1	$S_1$	0.09573	140.741	1470.148 *	22,691.17 1928.674	252,068.2 31,449.74	6,513,173.0 478,889.40
	$S_2$	0.03497	46.9133	1341.583	18,383.75 * 1560.902 *	204,746.0 * 25,523.47 *	5,295,918.0 * 389,275.30 *
	$S_3$	0.02212 *	31.2761 *	1413.831	21,670.09 1798.204	25,5421.1 31,249.22	6,760,883.0 493,758.50
2	$S_1$	0.01971 *	23.4570 *	1189.690 *	47,592.71 4707.847	378,100.2 53219.94	8,549,592.0 654,611.10
	$S_2$	0.16120	140.740	873.0723	26,107.70 * 2540.270 *	214,459.8 * 29,800.82 *	4,913,372.0 * 374,598.70 *
	$S_3$	0.06683	70.3699	1052.982	38,211.97 3559.850	343,929.2 46,187.47	8,167,798.0 615,707.70
3	$S_1$	0.03418 *	56.2962 *	1646.985 *	31,888.40 2705.927	355,665.3 44,315.56	9,204,857.0 676,491.80
	$S_2$	0.05094	70.3706	1381.427	21,872.89 * 1804.433 *	261,639.1 * 31,856.38 *	6,967,390.0 * 507,992.10 *
	$S_3$	0.09549	140.738	1473.826	22,734.82 1890.350	266,630.1 32,674.14	7,043,435.0 514,677.00

## 8. Concluding Remarks

This study takes into account the statistical inference of the unknown model parameters, reliability, and hazard rate functions of the inverted Nadarajah–Haghighi lifetime model based on generalized Type-II progressive hybrid censoring. The frequentist estimates with their asymptotic confidence intervals for the unknown parameters and any function of them were computed using the Newton–Raphson iterative procedure via the ‘maxLik’ package in  $\mathcal{R}$  software. Since the likelihood function was obtained in complex form, the posterior density function was obtained in nonlinear form. Therefore, using the Metropolis–Hastings algorithm, the Bayesian estimates and the associated HPD intervals were developed under the assumption of independent gamma priors and by considering the squared error loss function. To compare the behavior of the acquired estimates, various simulation experiments based on different choices of total test units, observed failure data, threshold times and progressive censoring plans were conducted, and they showed that the Bayes MCMC approach performed quite satisfactorily compared with the frequentist approach. Electronic devices and COVID-19 data sets were analyzed to show the practical utility of the proposed methods in real-life phenomenon and to suggest the optimum censoring plan. Finally, the Bayesian MCMC paradigm to estimate the parameters, reliability, and hazard functions of the INH distribution under generalized Type-II progressive hybrid censoring was recommended. We hope that the results and methodologies proposed here will be beneficial to reliability practitioners and extended to other censoring plans.

**Supplementary Materials:** The following supporting information can be downloaded at: <https://www.mdpi.com/article/10.3390/sym14112379/s1>, Table S1: The RMSEs (1st column) and MRABs (2nd column) of  $\alpha$ ; Table S2: The RMSEs (1st column) and MRABs (2nd column) of  $\delta$ ; Table S3: The RMSEs (1st column) and MRABs (2nd column) of  $R(t)$ ; Table S4: The RMSEs (1st column) and MRABs (2nd column) of  $h(t)$ ; Table S5: The ACLs of 95% ACI/HPD intervals of  $\alpha$ ; Table S6: The ACLs of 95% ACI/HPD intervals of  $\delta$ ; Table S7: The ACLs of 95% ACI/HPD intervals of  $R(t)$ ; Table S8: The ACLs of 95% ACI/HPD intervals of  $h(t)$ .

**Author Contributions:** Methodology, A.E. and O.E.A.-K.; funding acquisition, H.S.M.; software, A.E.; supervision H.S.M.; writing—original draft, H.S.M. and O.E.A.-K.; writing—review and editing, A.E. and O.E.A.-K. All authors have read and agreed to the published version of the manuscript.

**Funding:** This research was funded by Princess Nourah bint Abdulrahman University Researchers Supporting Project number PNURSP2022R175 from Princess Nourah bint Abdulrahman University in Riyadh, Saudi Arabia.

**Data Availability Statement:** The authors confirm that the data supporting the findings of this study are available within the article.

**Acknowledgments:** The authors acknowledge the support of Princess Nourah bint Abdulrahman University Researchers Supporting Project number PNURSP2022R175 from Princess Nourah bint Abdulrahman University in Riyadh, Saudi Arabia.

**Conflicts of Interest:** The authors declare no conflict of interest.

## Abbreviations

The following abbreviations are used in this article:

ACI	Approximate confidence interval
ACL	Average confidence length
Av.E	Average estimate
AVC	Asymptotic variance–covariance
CDF	Cumulative distribution function
COVID-19	Coronavirus disease
FP	Failure percentage
GPHCS-T2	Generalized progressive Type-II hybrid censoring scheme
HF	Hazard function
HPD	Highest posterior density
IL	Interval length
INH	Inverted Nadarajah–Haghighi
K-S	Kolmogorov–Smirnov
MCMC	Monte Carlo Markov chain
M-H	Metropolis–Hastings
MLE	Maximum likelihood estimator
MRAB	Mean relative absolute bias
NH	Nadarajah–Haghighi
PCS-T2	Progressive Type-II censoring
PDF	Probability density function
PHCS-T1	Progressive Type-I hybrid censoring scheme
PHCS-T2	Progressive Type-II hybrid censoring scheme
RF	Reliability function
RMSE	Root mean squared error
SE	Squared error
St.E	Standard error

### Appendix A

When differentiating Equation (7) with respect to  $\alpha$  and  $\delta$ , the elements of Equation (14) are as follows:

$$\mathcal{I}_{11} = \frac{D_\rho}{\alpha^2} + \sum_{j=1}^{D_\rho} (\phi_j^\alpha (\ln \phi_j)^2) - \sum_{j=1}^{D_\rho} R_j \frac{[1 - Z_j] [(\ln \phi_j)^2 Z_j (\phi_j^\alpha - \phi_j^{2\alpha})]}{[1 - Z_j]^2} - \frac{[\phi_j^\alpha \ln \phi_j Z_j]^2}{[1 - Z_j]^2} - \frac{\partial^2 \psi_\rho(T_\tau; \alpha, \delta)}{\partial \alpha^2},$$

$$\begin{aligned} \mathcal{I}_{22} = & \frac{D_\rho}{\delta^2} + (\alpha - 1) \sum_{j=1}^{D_\rho} x_j^{-2} \phi_j^{-2} + \alpha(\alpha - 1) \sum_{j=1}^{D_\rho} x_j^{-2} \phi_j^{\alpha-2} \\ & - \sum_{j=1}^{D_\rho} R_j \alpha x_j^{-1} \frac{[(1 - Z_j) [(\alpha Z_j x_j^{-1} \phi_j^{2\alpha-2}) (\phi_j^{-\alpha} - \alpha^{-1} \phi_j^{-\alpha} - 1)]]}{(1 - Z_j)^2} - [\alpha Z_j^2 x_j^{-1} \phi_j^{2\alpha-2}] \\ & - \frac{\partial^2 \psi_\rho(T_\tau; \alpha, \delta)}{\partial \delta^2}, \end{aligned}$$

and

$$\begin{aligned} \mathcal{I}_{12} = & - \sum_{j=1}^{D_\rho} x_j^{-1} \phi_j^{-1} + \sum_{j=1}^{D_\rho} x_j^{-1} \phi_j^{\alpha-1} (1 + \alpha \ln \phi_j) \\ & - \sum_{j=1}^{D_\rho} R_j \frac{(1 - Z_j) [(Z_j x_j^{-1} \phi_j^{\alpha-1}) (1 + \alpha \ln \phi_j - \alpha \phi_j^\alpha \ln \phi_j)]}{(1 - Z_j)^2} - [\alpha x_j^{-1} Z_j^2 \phi_j^{2\alpha-1} \ln \phi_j] \\ & - \frac{\partial^2 \psi_\rho(T_\tau; \alpha, \delta)}{\partial \alpha \partial \delta}, \end{aligned}$$

where

$$\begin{aligned} \phi_j &= \psi(\delta; x_j), Z_j = F(x_j; \alpha, \delta), \gamma_\tau = (1 + \delta T_\tau^{-1}), \frac{\partial^2 \psi_2(T_\tau; \alpha, \delta)}{\partial \alpha^2} = \frac{\partial^2 \psi_2(T_\tau; \alpha, \delta)}{\partial \delta^2} = \frac{\partial^2 \psi_2(T_\tau; \alpha, \delta)}{\partial \alpha \partial \delta} = 0, \\ \frac{\partial^2 \psi_\rho(T_\tau; \alpha, \delta)}{\partial \alpha^2} &= R_{D_\rho+1}^* \ln(\gamma_\tau) \frac{[(1 - \exp(1 - \gamma_\tau^\alpha)) (\gamma_\tau^\alpha \exp(1 - \gamma_\tau^\alpha) \ln \gamma_\tau) (1 - \gamma_\tau^\alpha)] - [(\gamma_\tau^\alpha)^2 (\exp(1 - \gamma_\tau^\alpha))^2 \ln \gamma_\tau]}{[1 - \exp(1 - \gamma_\tau^\alpha)]^2}, \\ \frac{\partial^2 \psi_\rho(T_\tau; \alpha, \delta)}{\partial \alpha \partial \delta} &= R_{D_\rho+1}^* \frac{[(1 - \exp(1 - \gamma_\tau^\alpha)) (\gamma_\tau^{\alpha-1} T_\tau^{-1} \exp(1 - \gamma_\tau^\alpha)) (1 + \alpha \ln \gamma_\tau - \alpha \gamma_\tau^\alpha \ln \gamma_\tau)] - [\gamma_\tau^{2\alpha-1} (\exp(1 - \gamma_\tau^\alpha))^2 \ln \gamma_\tau T_\tau^{-1}]}{[1 - \exp(1 - \gamma_\tau^\alpha)]^2}, \\ \text{and } \frac{\partial^2 \psi_\rho(T_\tau; \alpha, \delta)}{\partial \delta^2} &= \alpha R_{D_\rho+1}^* T_\tau^{-1} \frac{[(1 - \exp(1 - \gamma_\tau^\alpha)) (\gamma_\tau^{2\alpha-2} T_\tau^{-1} \exp(1 - \gamma_\tau^\alpha)) (\alpha \gamma_\tau^{-\alpha} - \gamma_\tau^{-\alpha} - \alpha)] - [\alpha T_\tau^{-1} \gamma_\tau^{2\alpha-2} (\exp(1 - \gamma_\tau^\alpha))^2]}{[1 - \exp(1 - \gamma_\tau^\alpha)]^2}. \end{aligned}$$

### References

- Chen, P.; Xu, A.; Ye, Z.S. Generalized fiducial inference for accelerated life tests with Weibull distribution and progressively type-II censoring. *IEEE Trans. Reliab.* **2016**, *65*, 1737–1744. [\[CrossRef\]](#)
- Xu, A.; Zhou, S.; Tang, Y. A unified model for system reliability evaluation under dynamic operating conditions. *IEEE Trans. Reliab.* **2019**, *70*, 65–72. [\[CrossRef\]](#)
- Hu, J.; Chen, P. Predictive maintenance of systems subject to hard failure based on proportional hazards model. *Reliab. Eng. Syst. Saf.* **2020**, *196*, 106707. [\[CrossRef\]](#)
- Luo, C.; Shen, L.; Xu, A. Modelling and estimation of system reliability under dynamic operating environments and lifetime ordering constraints. *Reliab. Eng. Syst. Saf.* **2022**, *218*, 108136. [\[CrossRef\]](#)
- Balakrishnan, N.; Cramer, E. *The Art of Progressive Censoring*; Birkhäuser: New York, NY, USA, 2014.
- Kundu, D.; Joarder, A. Analysis of Type-II progressively hybrid censored data. *Comput. Stat. Data Anal.* **2006**, *50*, 2509–2528. [\[CrossRef\]](#)
- Childs, A.; Chandrasekar, B.; Balakrishnan, N. Exact likelihood inference for an exponential parameter under progressive hybrid censoring schemes. In *Statistical Models and Methods for Biomedical and Technical Systems*; Vonta, F., Nikulin, M., Limnios, N., Huber-Carol, C., Eds.; Birkhäuser: Boston, MA, USA, 2008; pp. 319–330.
- Lee, K.; Sun, H.; Cho, Y. Exact likelihood inference of the exponential parameter under generalized Type II progressive hybrid censoring. *J. Korean Stat. Soc.* **2016**, *45*, 123–136. [\[CrossRef\]](#)
- Ashour, S.K.; Elshahhat, A. Bayesian and non-Bayesian estimation for Weibull parameters based on generalized Type-II progressive hybrid censoring scheme. *Pak. J. Stat. Oper. Res.* **2016**, *12*, 213–226.
- Ateya, S.; Mohammed, H. Prediction under Burr-XII distribution based on generalized Type-II progressive hybrid censoring scheme. *J. Egypt. Math. Soc.* **2018**, *26*, 491–508.

11. Seo, J.I. Objective Bayesian analysis for the Weibull distribution with partial information under the generalized Type-II progressive hybrid censoring scheme. *Commun.-Stat.-Simul. Comput.* **2020**, *51*, 5157–5173. [[CrossRef](#)]
12. Cho, S.; Lee, K. Exact likelihood inference for a competing risks model with generalized Type-II progressive hybrid censored exponential data. *Symmetry* **2021**, *13*, 887. [[CrossRef](#)]
13. Nagy, M.; Bakr, M.E.; Alrasheedi, A.F. Analysis with applications of the generalized Type-II progressive hybrid censoring sample from Burr Type-XII model. *Math. Probl. Eng.* **2022**, *2022*, 1241303. [[CrossRef](#)]
14. Nadarajah, S.; Haghighi, F. An extension of the exponential distribution. *Statistics* **2011**, *45*, 543–558. [[CrossRef](#)]
15. Tahir, M.H.; Cordeiro, G.M.; Ali, S.; Dey, S.; Manzoor, A. The inverted Nadarajah–Haghighi distribution: Estimation methods and applications. *J. Stat. Comput. Simul.* **2018**, *88*, 2775–2798. [[CrossRef](#)]
16. Elshahhat, A.; Rastogi, M.K. Estimation of parameters of life for an inverted Nadarajah–Haghighi distribution from Type-II progressively censored samples. *J. Indian Soc. Probab. Stat.* **2021**, *22*, 113–154. [[CrossRef](#)]
17. Henningsen, A.; Toomet, O. maxLik: A package for maximum likelihood estimation in R. *Comput. Stat.* **2011**, *26*, 443–458. [[CrossRef](#)]
18. Plummer, M.; Best, N.; Cowles, K.; Vines, K. coda: Convergence diagnosis and output analysis for MCMC. *R News* **2006**, *6*, 7–11.
19. Gelman, A.; Carlin, J.B.; Stern, H.S.; Rubin, D.B. *Bayesian Data Analysis*, 2nd ed.; Chapman and Hall/CRC: Boca Raton, FL, USA, 2004.
20. Lynch, S.M. *Introduction to Applied Bayesian Statistics and Estimation for Social Scientists*; Springer: New York, NY, USA, 2007.
21. Lawless, J.F. *Statistical Models and Methods for Lifetime Data*, 2nd ed.; John Wiley and Sons: Hoboken, NJ, USA, 2003.
22. Greene, W.H. *Econometric Analysis*, 4th ed.; Prentice-Hall: New York, NY, USA, 2000.
23. Chen, M.H.; Shao, Q.M. Monte Carlo estimation of Bayesian credible and HPD intervals. *J. Comput. Graph. Stat.* **1999**, *8*, 69–92.
24. Balakrishnan, N.; Aggarwala, R. *Progressive Censoring Theory, Methods and Applications*; Birkhäuser: Boston, MA, USA, 2000.
25. Ng, H.K.T.; Chan, P.S.; Balakrishnan, N. Optimal progressive censoring plans for the Weibull distribution. *Technometrics* **2004**, *46*, 470–481. [[CrossRef](#)]
26. Pradhan, B.; Kundu, D. Inference and optimal censoring schemes for progressively censored Birnbaum–Saunders distribution. *J. Stat. Plan. Inference* **2013**, *143*, 1098–1108. [[CrossRef](#)]
27. Elshahhat, A.; Abu El Azm, W.S. Statistical reliability analysis of electronic devices using generalized progressively hybrid censoring plan. *Qual. Reliab. Eng. Int.* **2022**, *38*, 1112–1130. [[CrossRef](#)]
28. Ashour, S.K.; El-Sheikh, A.A.; Elshahhat, A. Inferences and optimal censoring schemes for progressively first-failure censored Nadarajah-Haghighi distribution. *Sankhya A* **2022**, *84*, 885–923. [[CrossRef](#)]
29. Gupta, R.D.; Kundu, D. On the comparison of Fisher information of the Weibull and GE distributions. *J. Stat. Plan. Inference* **2006**, *136*, 3130–3144. [[CrossRef](#)]
30. Wang, F.K. A new model with bathtub-shaped failure rate using an additive Burr XII distribution. *Reliab. Eng. Syst. Saf.* **2000**, *70*, 305–312. [[CrossRef](#)]